COMPONENT PART NOTICE

THIS PAPER IS A COMPONENT PART OF THE FOLLOWING COMPILATION REPORT:

TITLE: Minutes of the Explosives Safety Seminar (22nd) Held in Anaheim, California on 26-28 August 1986. Volume 2.

TO ORDER THE COMPLETE COMPILATION REPORT, USE AD-A181 275.

THE COMPONENT PART IS PROVIDED HERE TO ALLOW USERS ACCESS TO INDIVIDUALLY AUTHORED SECTIONS OF PROCEEDING, ANNALS, SYMPOSIA, ETC. HOWEVER, THE COMPONENT SHOULD BE CONSIDERED WITHIN THE CONTEXT OF THE OVERALL COMPILATION REPORT AND NOT AS A STAND-ALONE TECHNICAL REPORT.

THE FOLLOWING COMPONENT PART NUMBERS COMPRISE THE COMPILATION REPORT:

AD#: P005 350 thru P005 393 AD#:

AD#: AD#:

AD#: AD#:

Accession For	
NTIS GRA&I	X
DTIC TAB	☐
Unannounced	☐
Justification	
By	
Distribution/	
Availability Codes	
Dist	Avail and/or Special
A-1	

VELOCITY MEASUREMENTS OF ACCEPTOR WALL FRAGMENTS FROM THE MASS DETONATION OF A NEIGHBORING ABOVEGROUND BARRICADED MUNITION STORAGE MAGAZINE MODEL

G. Bulmash
C. N. Kingery
G. A. Coulter

Ballistic Research Laboratory
Aberdeen Proving Ground, MD 21005-5066

(2W to the 1/3 power)

Abstract

This report presents the results of a study designed to determine if fragments from the most severely loaded wall of an aboveground brick munition storage magazine would cause a mass detonation of the munitions within the magazine. Unreinforced, scored concrete of similar density was substituted for brick in the wall of the acceptor. The blast loading is the result of a mass explosion in a neighboring magazine which is located at a separation distance of K2 ($2W^{1/3}$); the magazines are separated by earth barricades. Responding and non-responding 1/23.5 scaled models were designed for the tests. Velocity measurements were obtained by using voltage interrupt wire screens. It was determined that the maximum fragment velocity, 10.8 m/s, is too low to initiate a sympathetic detonation.

I. INTRODUCTION

This study was sponsored and funded by the Department of Defense Explosive Safety Board (DDESB). In Machrihanish, Scotland munitions are stored in aboveground brick magazines that are surrounded on three sides by earth barricades and located at a separation distance of K2 ($2W^{1/3}$). The U.S. Navy stores weapons in this facility. It is the purpose of this report to determine if a mass explosion in one magazine, the donor, would result in a sympathetic mass explosion in the nearest neighbor magazine, the acceptor. The direct cause of a mass explosion in the acceptor would be high velocity fragments from the acceptor wall.

In the test procedure section of this report will discuss the scaling and simplifying assumptions used to go from the full scale Machrihanish site to a feasible test layout. This section will also cover the design and construction of the concrete donor magazine, the concrete acceptor wall, and the steel nonresponding models. Static and dynamic tests to establish the strength of the concrete acceptor wall will be discussed as well as dynamic shock tube tests on the acceptor wall that approximate the blast loading expected in the field tests. The instrumentation used to measure blast pressures and wall fragment velocities will be described, and the test layout and firing program will be presented.

The results section will first present the field blast data, and show it is reasonable and consistent. Data establishing the concrete acceptor wall strength will be presented. Preliminary velocity data from the shock tube velocity tests will be discussed. Fragment velocity data from the field tests will be reduced and analyzed. It will be shown that the fragment velocities measured in this study are less than those calculated when the same blast loads are applied to unbounded fragments. This is the upper limit on the velocity. Comparisons with other model studies concerning fragment or debris velocities will be presented.

Finally, the report will conclude that the maximum velocity obtained, 10.8 m/s, is too low to initiate a sympathetic detonation. A busy reader who has faith and is interested in results may proceed to Section III D, "Field Tests Fragment Velocities," where the essence of this report is presented.

II. TEST PROCEDURE

A. Scaling and Simplifications

The Machrihanish magazines of interest are brick and concrete structures 9.67 x 7.82 x 3.65 meters. The walls are composed of a double layer of brick with an air cavity between the layers; the floor and ceiling are made of concrete. These magazines contain a mixed explosive load, typically mines, torpedoes, and destructors (Reference 1).

The authorized mass of high explosives that may be contained in the Machrihanish magazines that are being studied is 13,000 kg (Reference 1). Kingery made the conservative assumption that 13,000 kg of mixed explosives could be modeled with an equivalent amount of Pentolite (Reference 2). The 13,000 kg full scale charge weight was scaled to a one kg bare, hemispherical Pentolite charge for this experiment. Applying cube root scaling, a one kg test charge results in a 1/23.5 scale model; the donor, acceptors, and barricades are 1/23.5 scale.

The Machrihanish magazines are simple structures designed to protect munitions from the weather and allow for quick access. However, attempting to model the strength of even these basic structures on a 1/23.5 scale was impractical. The best approach was to scale the mass by constructing the responding models of similar materials*.

B. Models

Three scale models were designed for this program: a responding concrete donor structure, a nonresponding acceptor model instrumented with piezoelectric transducers, and a nonresponding steel acceptor with one responding concrete wall.

1. Concrete Donor Model. The concrete donor model, which is used to simulate a mass explosion in a full scale magazine, is composed of five separate concrete slabs and a cardboard door. The cardboard door simulates the relatively unsubstantial door in the real magazine, a door designed to readily fail and focus the blast forward away from neighboring magazines. Refer to Figure 1, a photograph showing the floor, walls, and roof; the door is not present. Also evident on Figure 1 is a small hole for emplacing the detonator and a groove for the detonator wire. The one kg bare Pentolite charge is centered on this hole. These slabs were poured in small wooden forms, and copper wire was placed in the soft concrete in a criss-cross pattern. The rebar was used to prevent the slabs from breaking while being handled. The slabs were made from "Sakrete Sand Mix;" gravel could not be incorporated in the mixture because the stones have a larger diameter than the slab thickness. The roof has the minimum thickness of 0.64 cm, and the floor has the maximum thickness of 1.27 cm. To create a complete donor structure, the slabs and door were placed together. The parts stood on their own; no binding material was used to hold this model together.

In creating this donor magazine model no attempt was made to explicitly match the strength of the full scale magazine. Sand based concrete mix was used because it has a density approximately equal to that of the brick and concrete in the original structure. In this manner, the dimensions and mass were both scaled by 1/23.5. The density of the brick walls in the Machrihanish magazines is 1,910 kg/m^3, and the density of the concrete roof is 2,224 kg/m^3 (Ref. 1). A sample of the concrete models had a density of 1,959 $\pm$206 kg/m^3.

* W. E. Baker, Wilfred Baker Engineering, San Antonio, TX, August 1984, private communication).

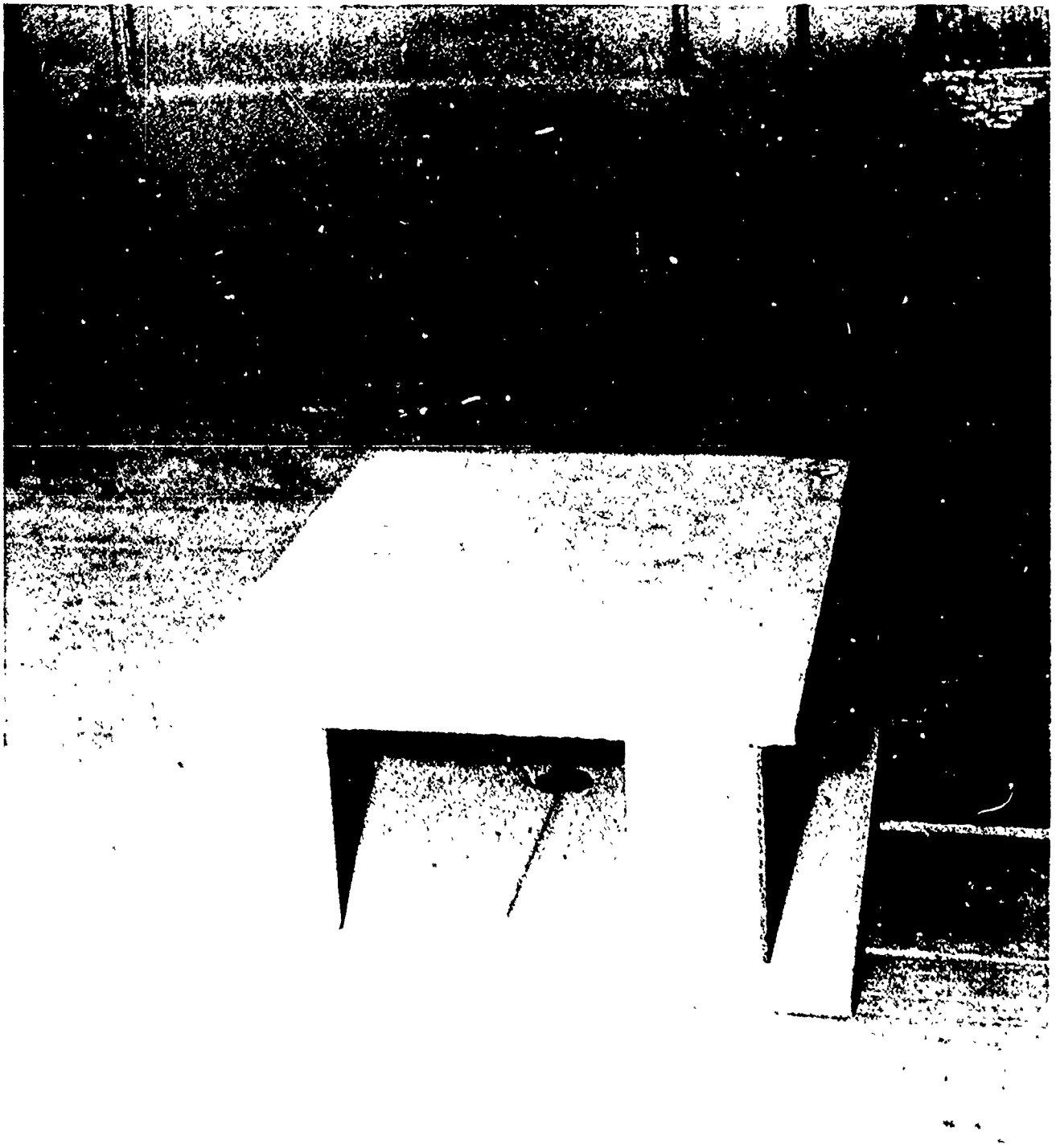

Figure 1. Photograph of Concrete Donor Model

2. Steel Nonresponding Acceptor Model. The purpose of this model is to document the blast loading experienced by the responding concrete wall that will be discussed in Section 3. Dimensions of the steel acceptor model are 30.5 x 33.3 x 41.1 cm (see Figure 2). The model was constructed from 2.54 cm thick steel plate. All surfaces are welded together except for the front wall which was bolted to the model to facilitate emplacing gages, wires, and connectors. For stability the acceptor extends 15 cm below ground level. Therefore, the exposed dimensions are 15.5 x 33.3 x 41.1 cm. There are 5 transducer positions on the model: four on the near sidewall, which experiences the most severe blast loading, and one on the roof. In Figure 2, the five gage positions are labelled 2 through 6.

3. Nonresponding Steel Acceptor Model with One Responding Concrete Wall. The heart of this experiment is the measurement of velocities of fragments from the responding acceptor wall. The concrete acceptor wall is supported by a nonresponding steel acceptor similar to the model described in Section 2. Refer to Figures 3 and 4, a sketch and photograph of this model. This acceptor is also constructed from 2.54 cm steel. In this case, all surfaces are welded together, except for the roof which is bolted to allow for emplacing velocity measurement screens and their supporting structure.

The concrete wall is placed against this steel acceptor as indicated on Figures 3 & 4. It is rigidly supported by the steel side walls of the acceptor and for most shots is attached to the floor and overlapping roof with caulking material. The concrete wall was constructed from the same sand mix used to create the donor structure discussed in Section 1. Reinforcing wire was not used in this 0.9 x 12.7 x 40.6 cm wall. A PCB gage (PCB Electronics Inc. piezoelectric pressure transducer) was placed adjacent to the wall. This is gage position 1; its location is indicated on Figure 4.

Optionally, with the concrete wall removed, 2.54 cm and 1.27 cm diameter concrete plugs 0.9 cm thick could be tested by placing them in a nonresponding steel plate containing two mounting holes. This plate bolts to the side of the steel acceptor as indicated on Figure 5. In this arrangement it was possible to obtain velocity measurements without using blast energy to break up the the responding target. A PCB gage was placed in the center of the plate. This is gage position 1 as indicated on Figure 5.

Although modeling the strength of the full scale wall explicitly was not feasible, it was imperative that the model wall not be too strong. A wall that was excessively strong would consume too much of the blast energy in breaking up, and the consequent fragment velocities would be unrealistically low. For this program it was determined that the wall should fail at approximately 34.5 kPa (5 psi). Two unreinforced brick houses were subjected to nuclear blasts at the Nevada Test Site in 1955 (Reference 3). The building placed at the 11.7 kPa level was structurally intact after the test whereas the one at the 34.5 kPa level was destroyed with most of the debris remaining nearby.

Another important consideration in designing this wall was the break

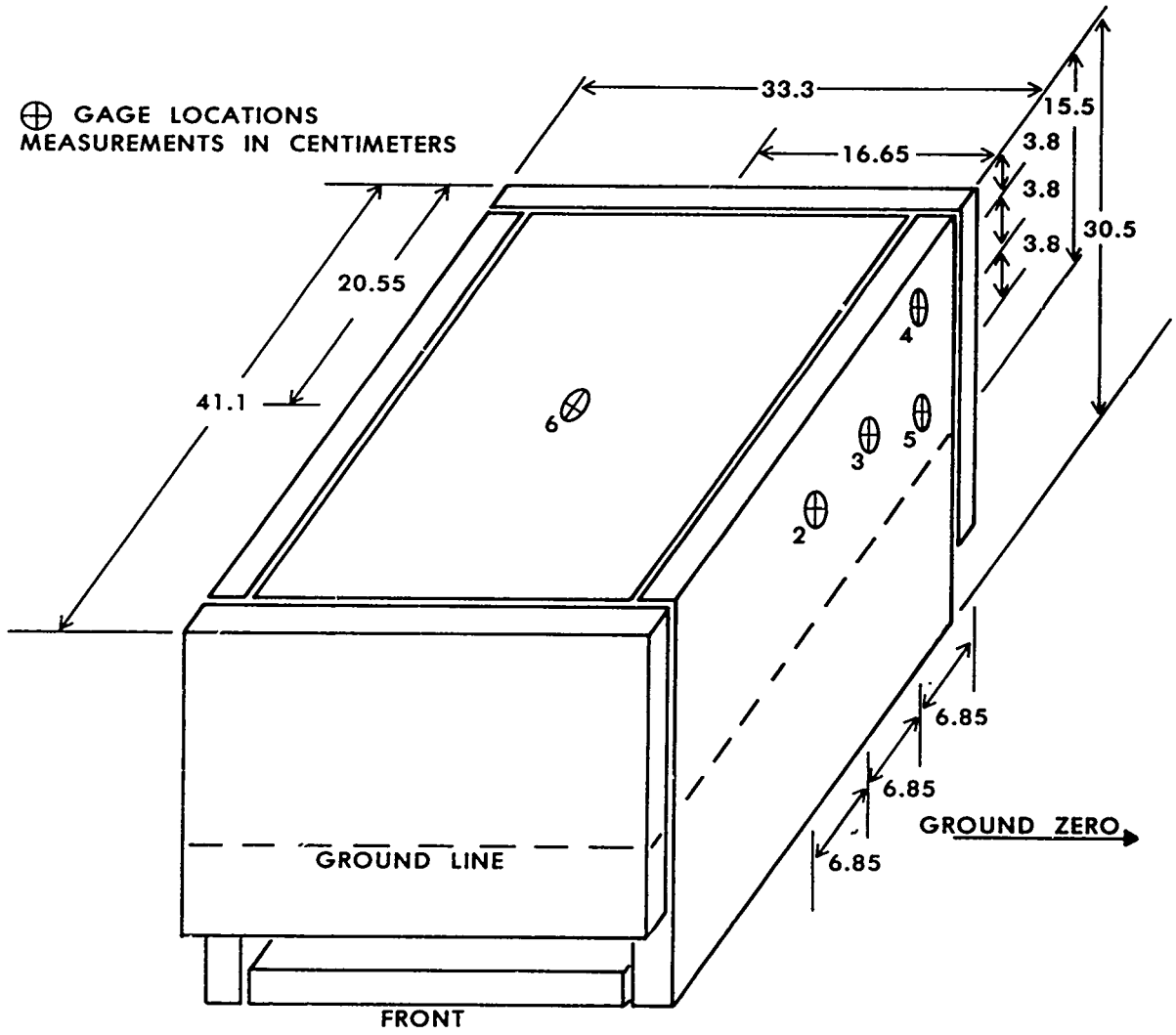

Figure 2. Nonresponding Acceptor Model

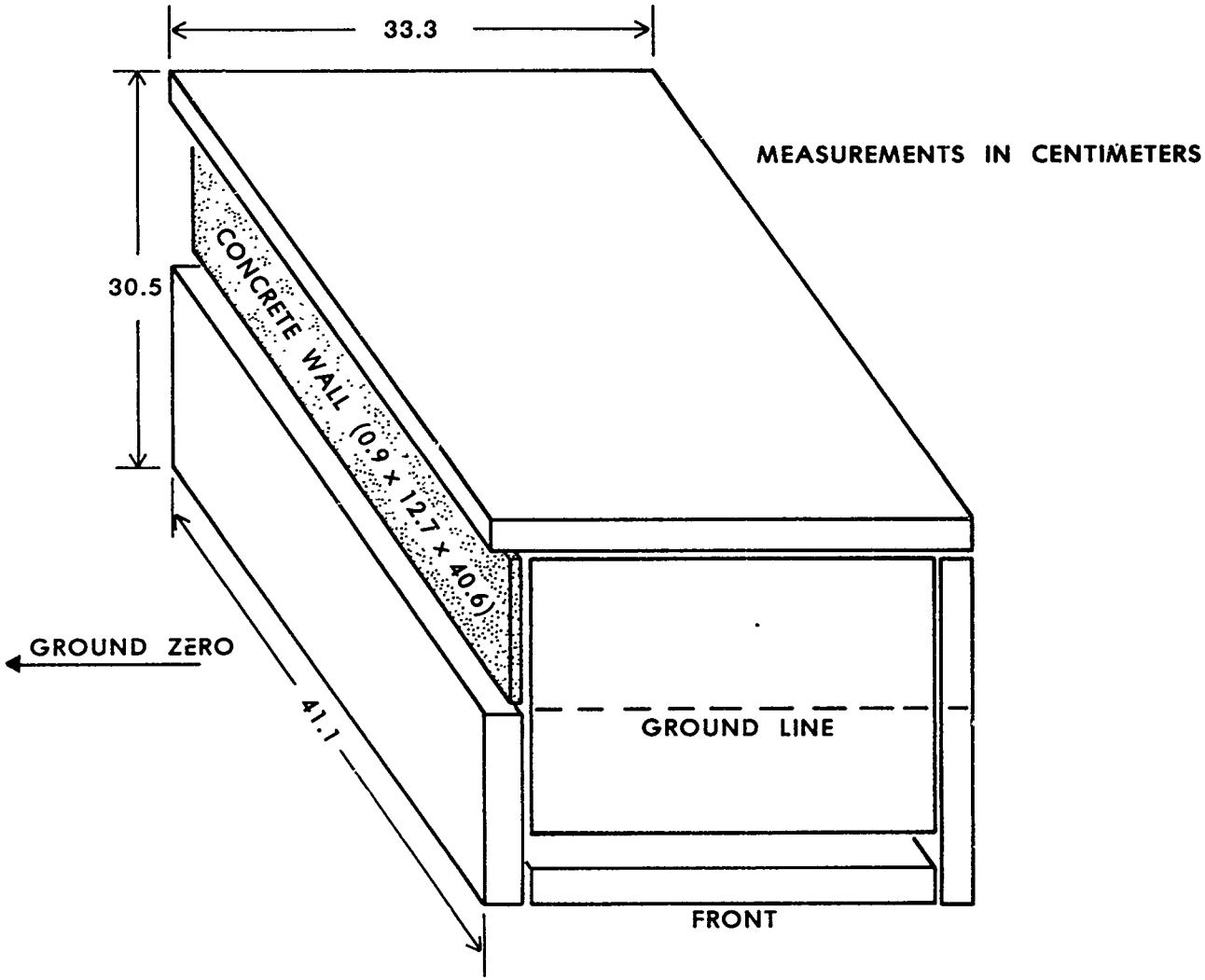

Figure 3. Sketch of the Acceptor Model with One Responding Concrete Wall

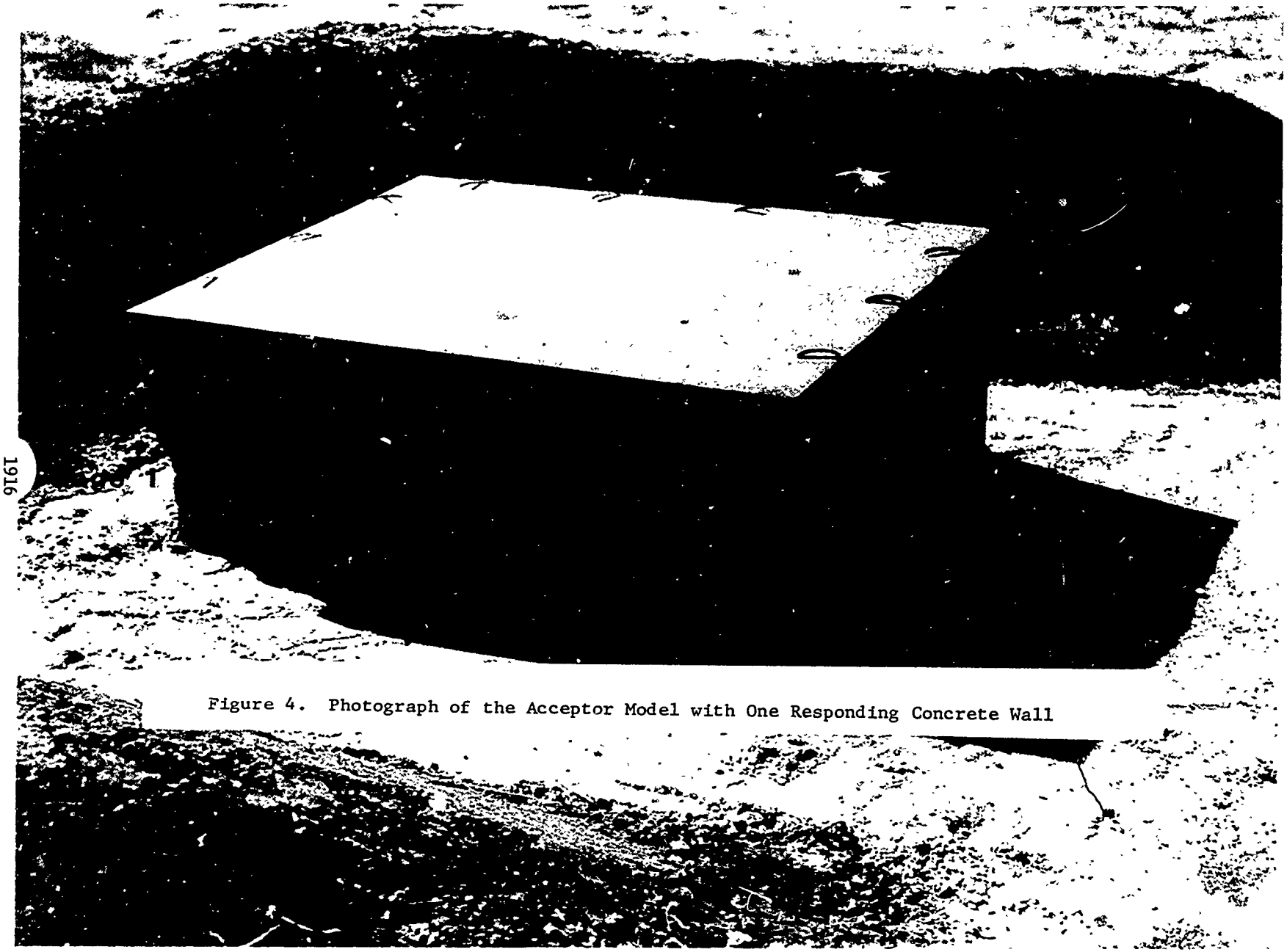

Figure 4. Photograph of the Acceptor Model with One Responding Concrete Wall

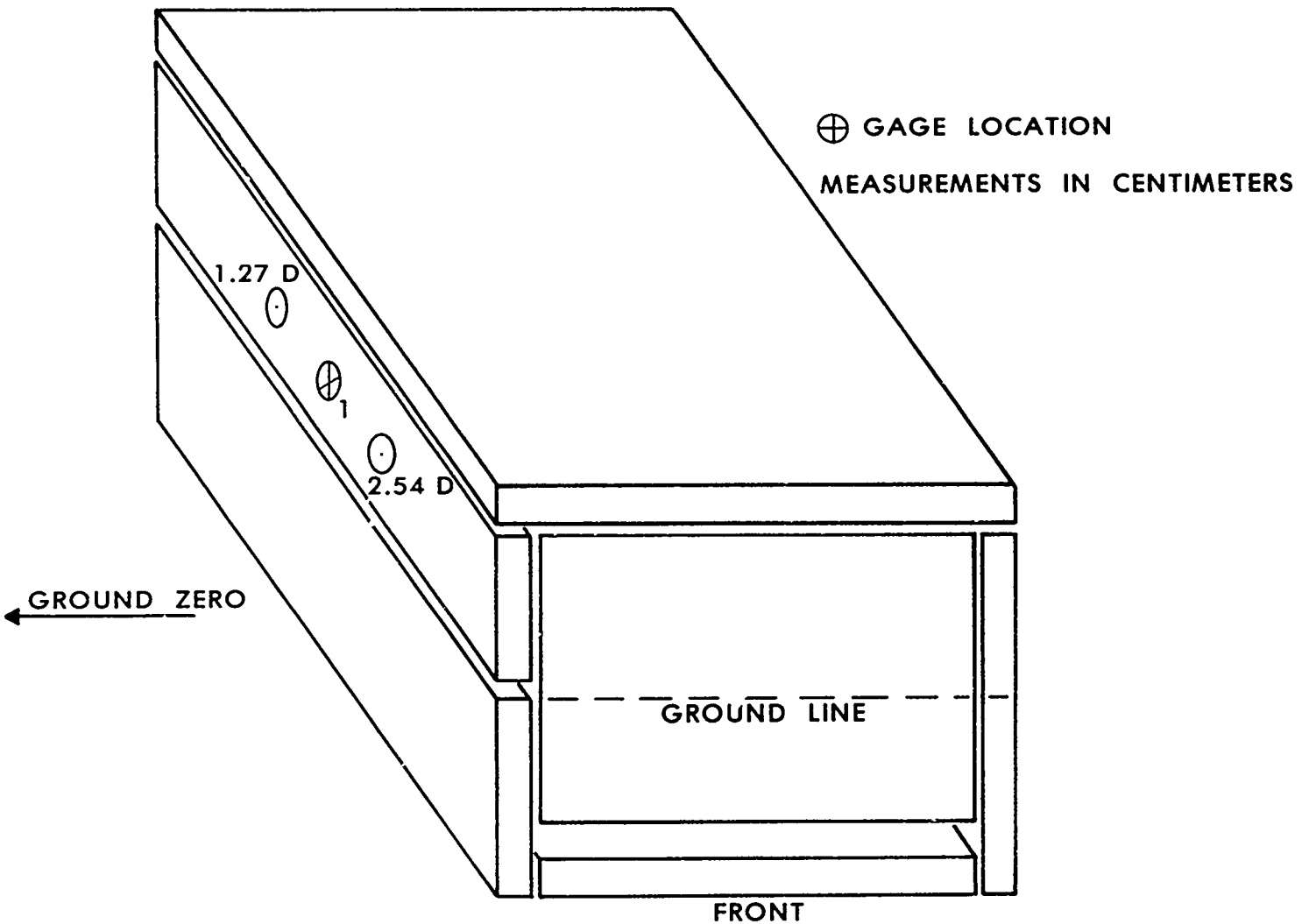

Figure 5. Acceptor Model with a nonresponding Steel Plate Containing Holes for Two Concrete Plugs

up pattern. The wall was scored to break up into regular 2.54 x 2.54 cm squares; the break up pattern was finalized after the strength tests discussed in Section 4. This size corresponds to full scale fragments that are 0.60 meters square, 0.21 meters thick and weigh 147.5 $\pm$15.5 kg. Preliminary shock tube velocity tests on concrete acceptor walls showed that an unscored wall broke up into fragments having irregular size and shape. These tests are discussed in Section C.

4. Tests to Determine the Strength of the Concrete Acceptor Wall. These tests were an essential part of the wall design.

a. Quasi-static Tests. An Instron model TTM hydraulic loading machine was used to apply a quasi-static, uniformly distributed load to a number of the concrete acceptor walls. A Starrett displacement gage was attached to the underside of the wall to simultaneously measure displacement as a function of loading. Figure 6 shows the quasi-static test arrangement. For these tests the wall was simply supported by a wood frame that overlapped the concrete by 1.27 cm on all four sides.

b. Dynamic Tests. The BRL 10.2 x 38.1 cm compressed air shock tube (Reference 4) was used to apply a dynamic load to a number of the concrete walls. Figure 7 is an illustration of this test setup. A wall was situated between two sections of the shock tube and held in place hydraulically. In this arrangement the wall was clamped and the shock tube overlapped the concrete by 1.27 cm on all four sides. These dynamic tests were performed with three different shock tube compression chamber lengths: 147.3 cm, 45 ~ cm, and 8.3 cm. The length of the compression chamber or driver determined the shock wave positive phase duration and affected the impulse. By varying the driver length and compression chamber pressure, the wave shape was manipulated in an attempt to simulate a free field blast wave which characteristically exhibits exponential decay and, for a one kg charge, short duration (0.7 msec in the field tests). Each wall was tested at very low overpressure and examined for failure. The pressure was increased incrementally and the wall reexamined after every test until the wall failed. The walls were mounted normal to the shock flow and exposed to full reflected pressure.

Pressure-time records were obtained by placing one or two PCB Electronics Inc. model 113A piezoelectric transducers in the shock tube. One of these gages, which was used on every shot, was mounted against the shock tube wall 58.4 cm upstream from the test location to record the side-on pressure. The other gage was used to determine the full reflected pressure load that the concrete wall would experience. It was mounted in the center of the steel plate described in Section B 3. This steel plate was placed at the test location instead of the concrete wall. A series of shots was fired to determine the reflected pressure at the test location. Then the plate was removed and replaced with the concrete wall. When tests were performed on the concrete wall, only the upstream side-on gage was present. In this way it was possible to correlate the side-on pressures obtained when the plate and wall were tested with the reflected pressure on the plate. Thus, the reflected pressure on the wall was determined. The pressure-time records were stored in a Tektronix 5223 digitizing oscilloscope and transferred to a Tektronix 4051 microcomputer for analysis.

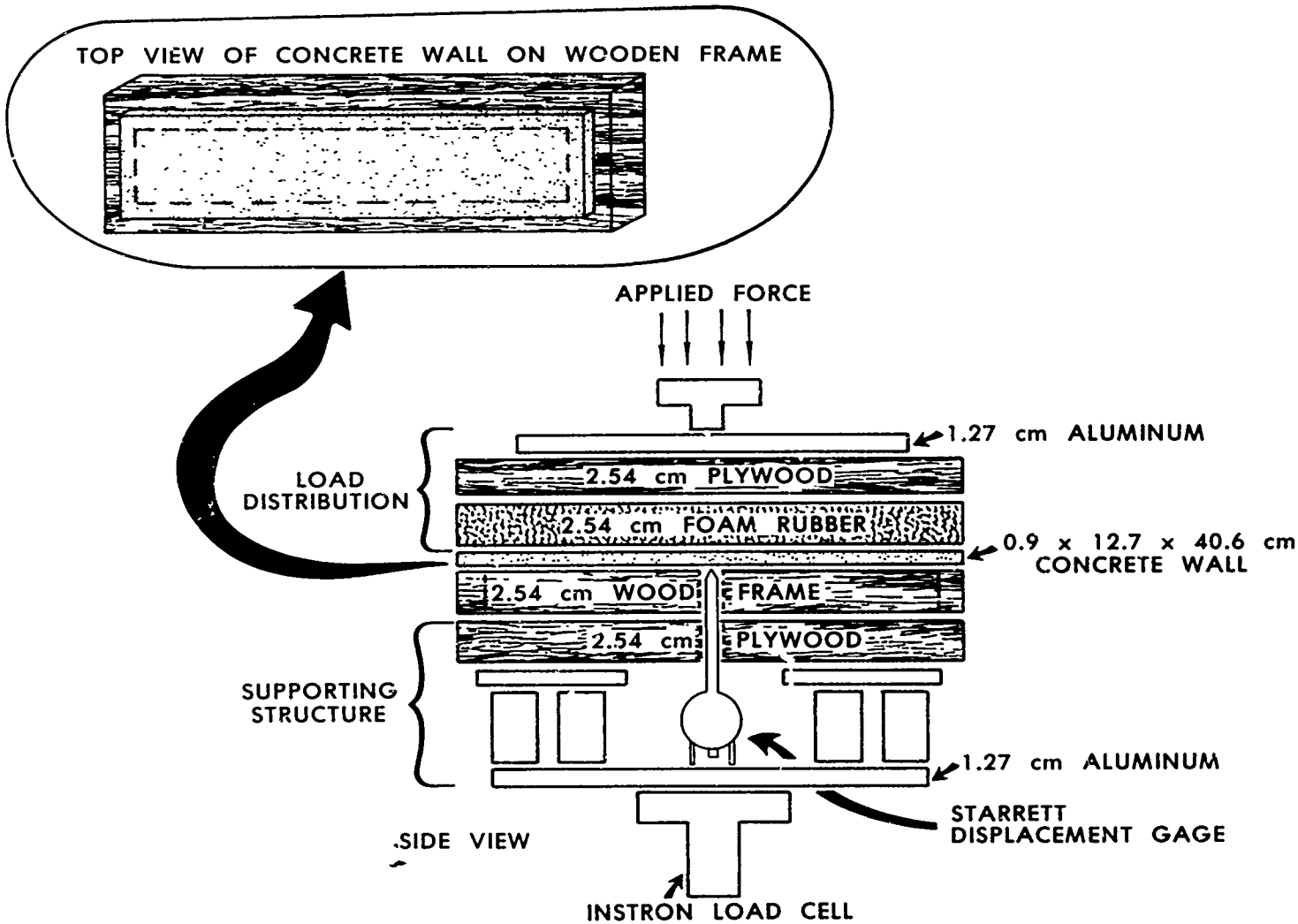

Figure 6. Quasi-static Loading Arrangement Used to Establish Concrete Acceptor Wall Strength

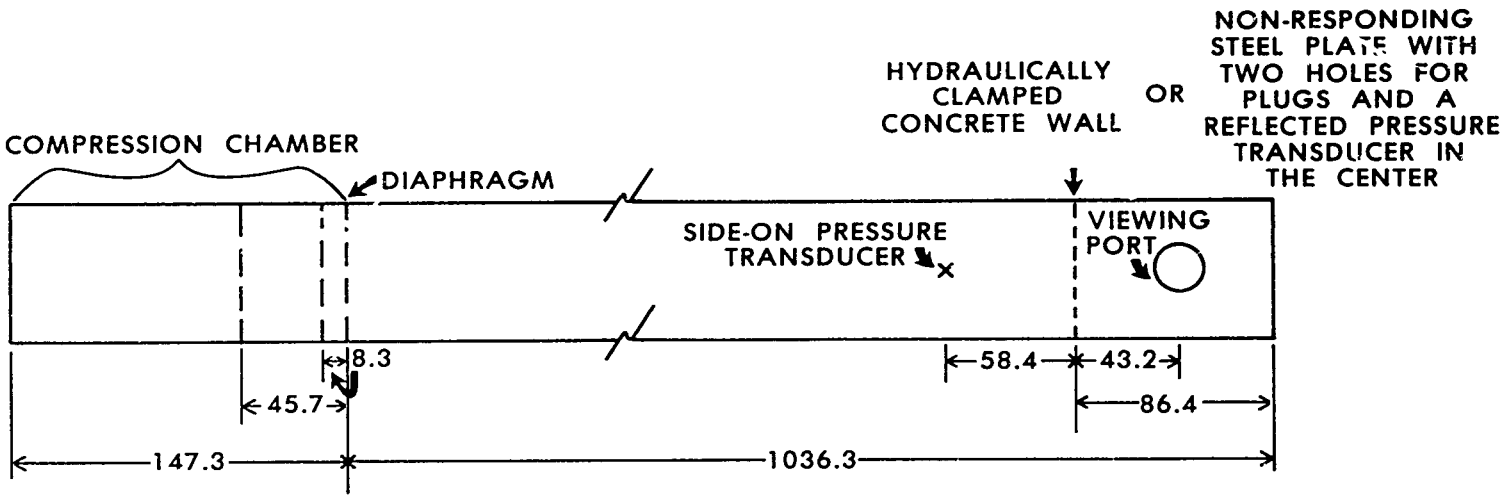

Figure 7. BRL 10.2 x 38.1 cm Compressed Air Shock Tube Setup for a Concrete Wall Test

C. Shock Tube Velocity Tests

Shock tube tests were performed to develop an approximation of the fragment velocities expected in the field tests. Employing the same arrangement discussed in Section 4 b above, a number of concrete walls were tested dynamically in the 10.2 x 38.1 cm shock tube at overpressures that caused them to fail and send fragments downstream with measurable velocities. These tests were performed using an 8.3 cm driver. Velocity measurements were obtained at a glass port located 43.2 cm downstream from the concrete wall test site. A 16 mm high speed camera, operating at 1000 frames per second, photographed the fragments as they passed the port. Additionally, a 2.54 cm diameter concrete plug 0.9 cm thick was tested in the shock tube by placing it in a nonresponding steel plate containing a small mounting hole. This is the same plate that attaches to the steel nonresponding model discussed in Section B 3 (refer to Figure 5). The concrete plug was placed in the mounting hole but was not secured. Thus, no blast energy was required to free the plug, and the measured velocity is an upper limit achievable in this test arrangement.

D. Field Tests

The field tests were performed during March 1985 at the Ballistic Research Laboratory outdoor Range 8 located on Spesutie Island, Aberdeen Proving Ground. Previous work, sponsored by the DDESB and performed by the BRL, concerned with the Machrihanish storage facility is reported in references 2 and 5.

1. Test Instrumentation. The pressure recording and velocity measurement instrumentation are described in this section.

a. Pressure Recording Instrumentation. The instrumentation for this test series consisted of pressure transducers, a magnetic tape recorder, and a data reduction system. A block diagram is shown on Figure 8. PCB Electronics Inc. model 113A piezoelectric pressure transducers, having quartz sensing elements and built-in source followers, were used to obtain pressure-time records of the blast event. The Honeywell tape recorder consists of three basic units: a power supply and voltage calibrator, amplifiers, and an FM recorder having a 80 kHz response time. A Honeywell Visicorder oscillograph with 5 kHz response was used for preliminary analysis of the pressure records. Data was processed through an analog to digital converter and transferred to a Textronix 4052 microcomputer that was used to create working plots. Finally, the data was transferred to linked CDC Cyber 750 and 7600 mainframe computers for further analysis.

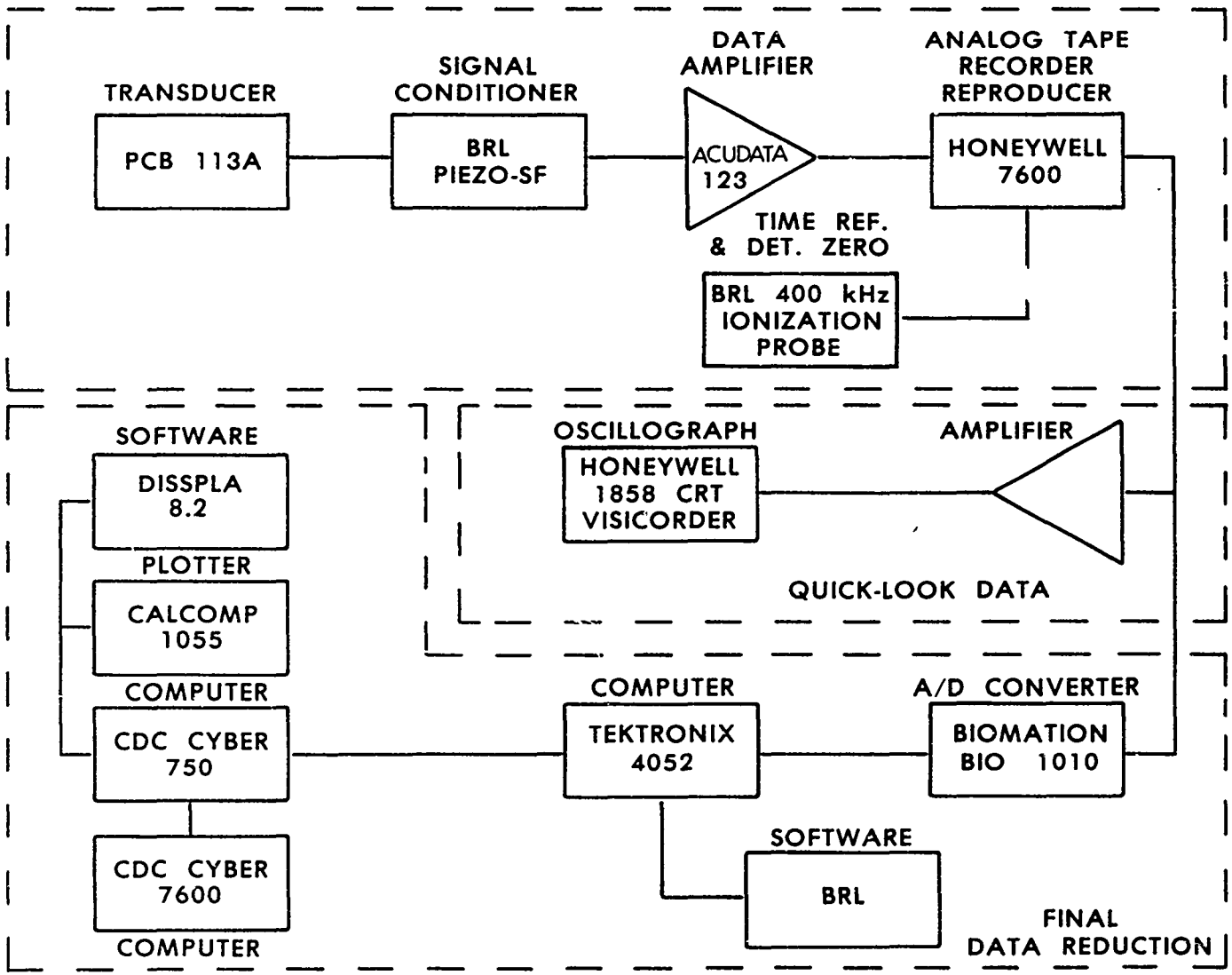

Figure 8. Data Acquisition/Reduction System

b. Velocity Measurement Instrumentation. Velocity measurements were obtained by using a variation of the voltage interrupt or "break screen" method. A break screen is a piece of thin paper coated with an electrically conducting chemical to create a circuit. When a fragment strikes the paper, it interrupts the circuit and a time measurement may be recorded on a digital counter. By placing two break screens within the nonresponding acceptor, one behind the other, concrete wall fragment velocities may be calculated from the start and stop times recorded on a counter and the known distance between the break screens, in theory. However, in early field tests, extraordinarily high velocities were obtained using this method. These velocities, in the range 200-341 m/s, were attributed to the ground shock. The blast event propagates a shock, through the solids on the test site, to the break screens which interrupts the circuits. Realistic fragment velocity measurements were obtained by replacing the paper break screens with single strand wire. Figure 9 displays the velocity measurement setup within the steel acceptor model. Even the thinnest wire offered mechanical resistance to the advancing fragments; this slowed the fragments down. Therefore, a method was required to start the counters without reducing the velocities. A PCB gage, placed adjacent to the concrete wall, was used as the start signal. Notice that there is a second set of looped wire circuits in the background. Velocities recorded here were lower than on the first set of circuits, because breaking the wires impeded the fragments. Measurements from the background circuits were not used.

Figure 10 is a block diagram of the velocity measurement system. The PCB gage is the start source for the Racal-Dana counter, and the wire circuit stops the counter when the wire is cut by a fragment.

2. Test Layout. A diagram and photograph of the test layout are presented on Figures 11 and 12. The entire test site, that is, the barricades, donor and acceptors, is 1/23.5 scale. The barricades are composed of compacted soil, and the test pad is coarse sand. The steel acceptors, which remained in place for all nine shots, were stabilized in several ways. The lower 15.2 cm of the walls were buried in the sand. Four steel straps were placed across and around the floor of each acceptor, and the straps were secured with 61.0 cm spikes driven into the test pad.

The test pad configuration is symmetric about an axis going through the free field gage (Station 7 on Figure 11) and the center line of the donor. Because of this symmetry, the blast loading on both steel acceptors should be the same; four gages on the near wall of the nonresponding acceptor should measure the blast loading experienced by the concrete wall on the other acceptor.

3. Firing Program. Nine test shots were fired during the period 11 March - 27 March 19 - at Range 8 on Spesutie Island. For a concise summary of the firing program, refer to Table 1. On Shots 1 and 2 the concrete plugs were tested. On Shots 3 - 8 the concrete walls were tested. On Shot 9 the plugs were again tested, this time with the barricades removed.

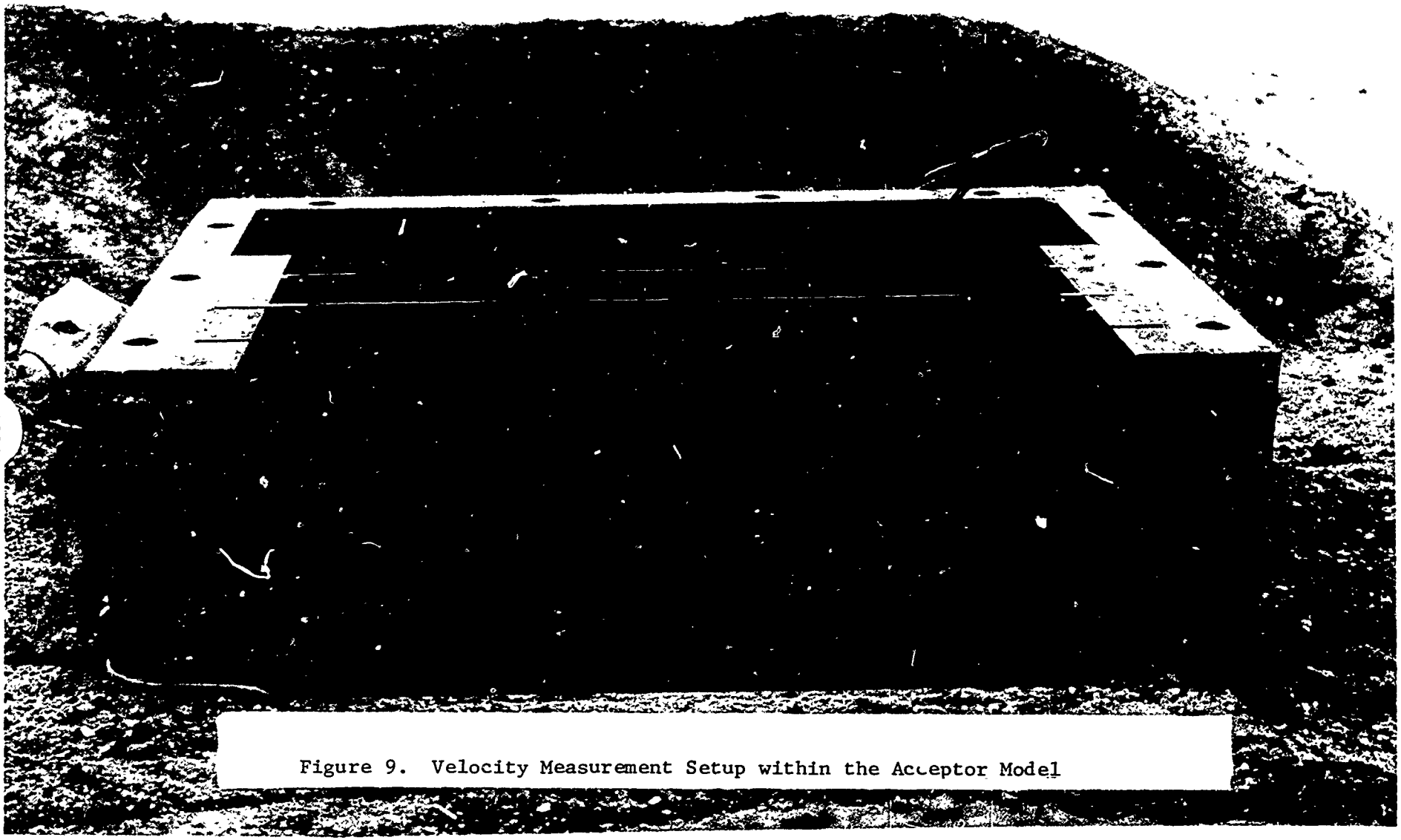

Figure 9. Velocity Measurement Setup within the Acceptor Model

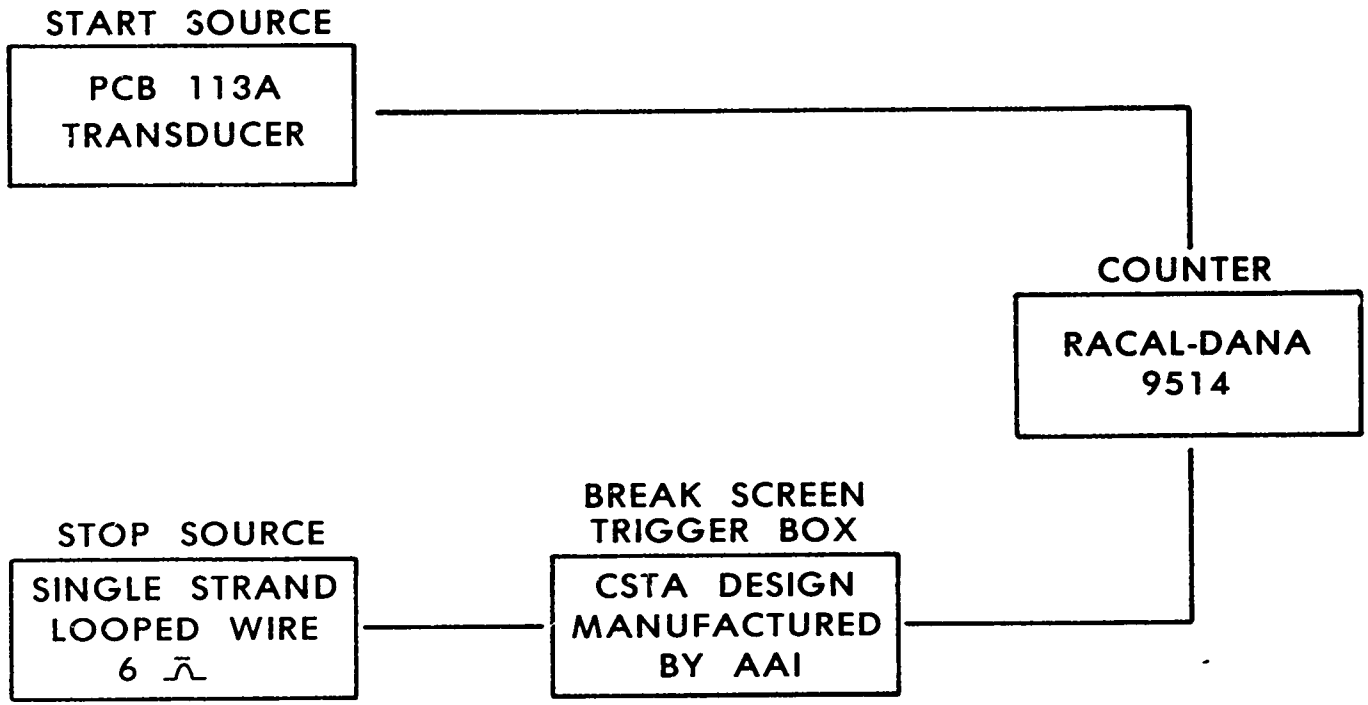

Figure 10. Block Diagram of the Velocity Measurement System

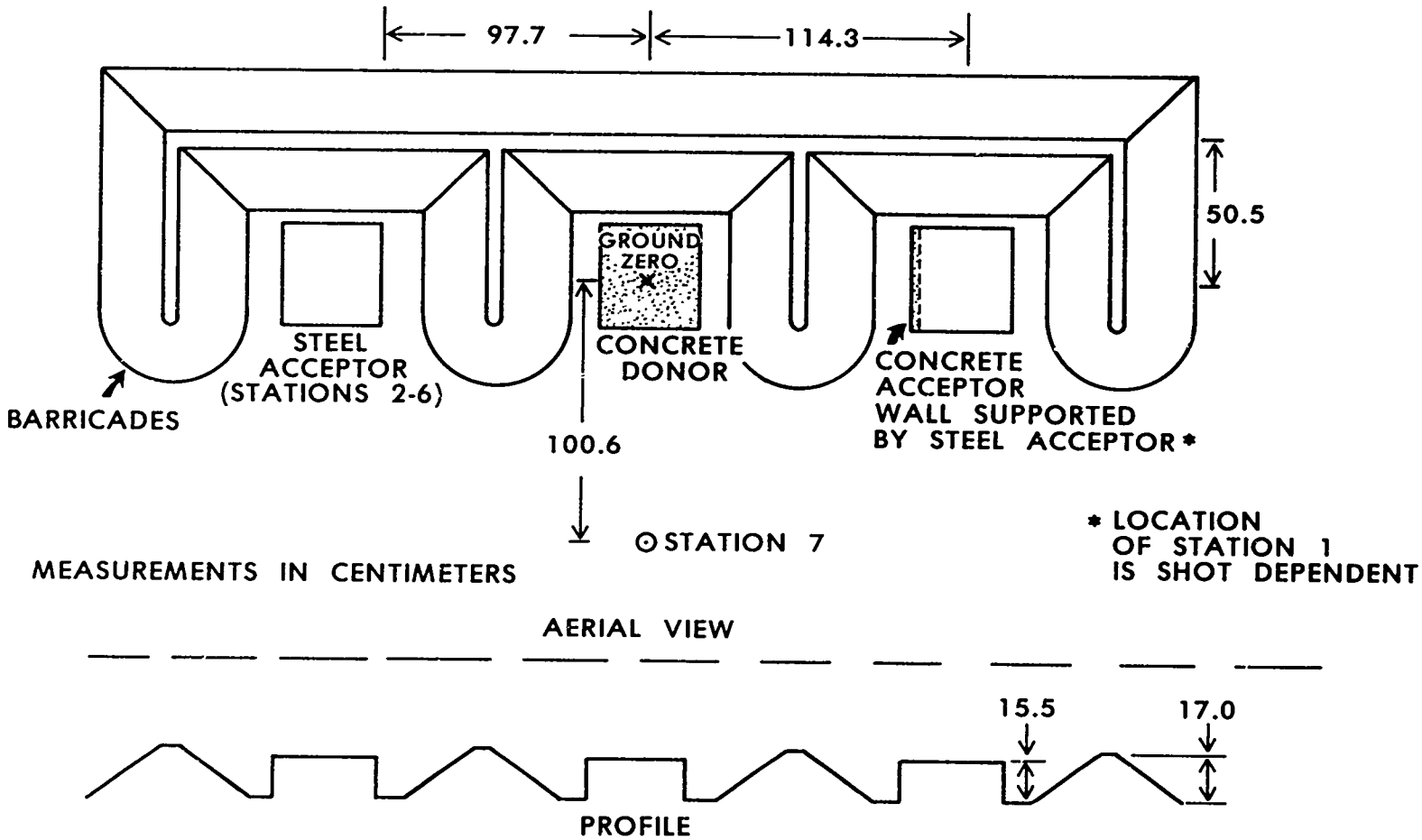

Figure 11. Diagram of the Test Layout

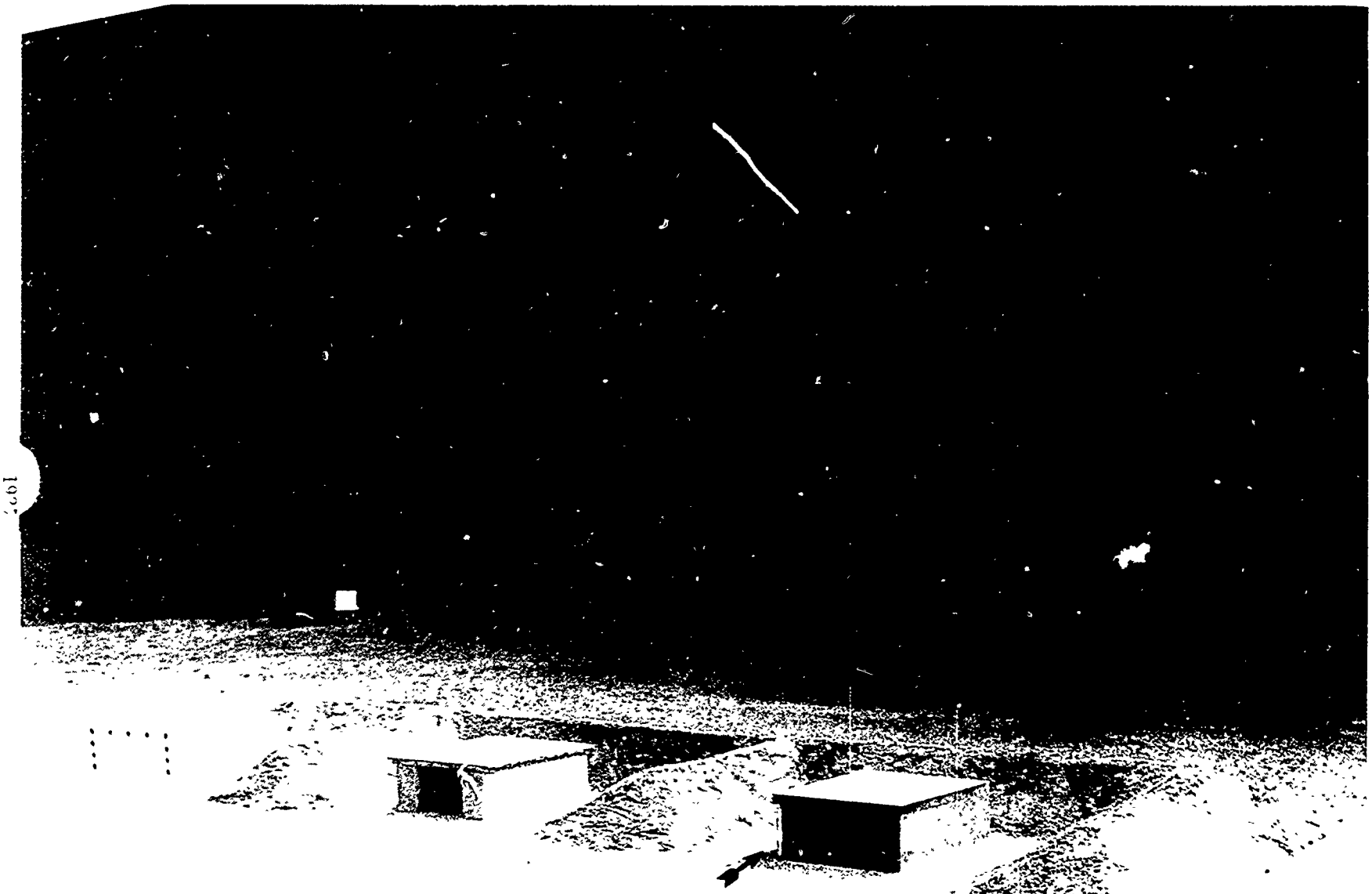

Figure 12. Photograph of the Test Site

TABLE 1. FIRING PROGRAM

Shot#	Concrete Target	Velocity Instrumentation	Barricades
1	Plugs	Paper Screens	Yes
2	Plugs	Paper Screens	Yes
3	Wall	Wire	Yes
4	Wall	Wire	Yes
5	Wall	Wire	Yes
6	Wall	Wire	Yes
7	Wall	Wire	Yes
8	Wall	Wire	Yes
9	Plugs	Wire	No

III. RESULTS

A. Field Test Blast Data

The acceptor sidewall nearest to the blast experiences the most severe load (Ref. 2). An interpretation of the blast loading on the near sidewall and roof of the acceptor is presented on Figure 13. The shock front strikes the near sidewall at a 33.9 degree angle whereas it strikes the roof at an angle of 56.1 degrees causing the roof to experience a lower loading. Because of the higher loading, the near sidewall is the focus of this study.

The pressure-time (P-T) records for all seven stations from Shot 2 are displayed in Figure 14. Station 1 is located in the center of the nonresponding plate (see Figure 5); this corresponds to the center of the concrete wall. Likewise, Station 2 (see Figure 2) is located at the center of the near wall on the nonresponding steel acceptor. Because of the test site symmetry, Stations 1 & 2 should undergo the same loading. Fragments from the center of the concrete wall have the highest velocities; Station 1 & 2 are of primary interest. Station 3-5 are also located on the nonresponding acceptor's near wall as indicated on Figures 2. Station 6, on the roof is subjected to a much lower load. Station 7 is located 100.6 cm in front of ground zero. The gage at Station 7, mounted flush

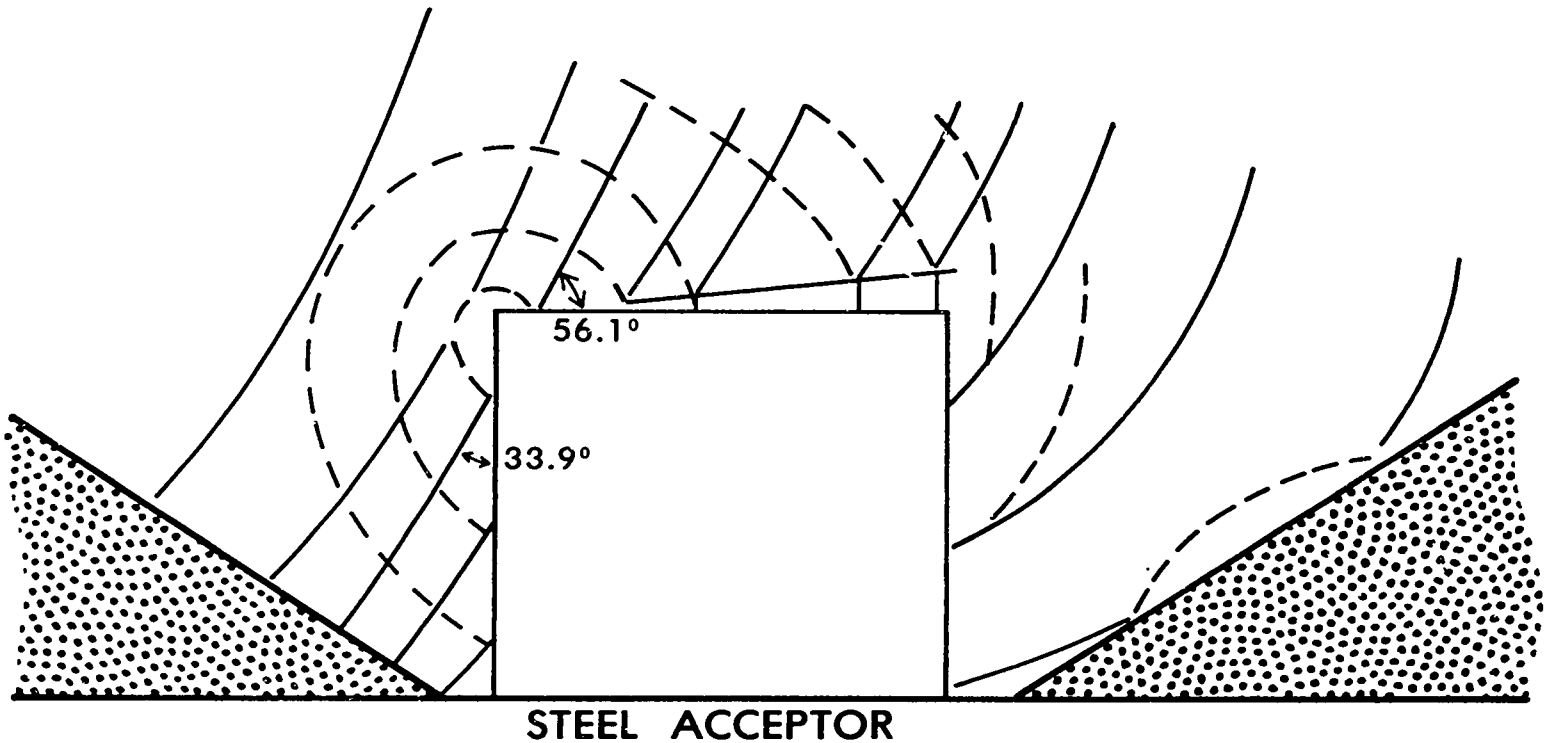

Figure 13. Shock Loading on Acceptor Models

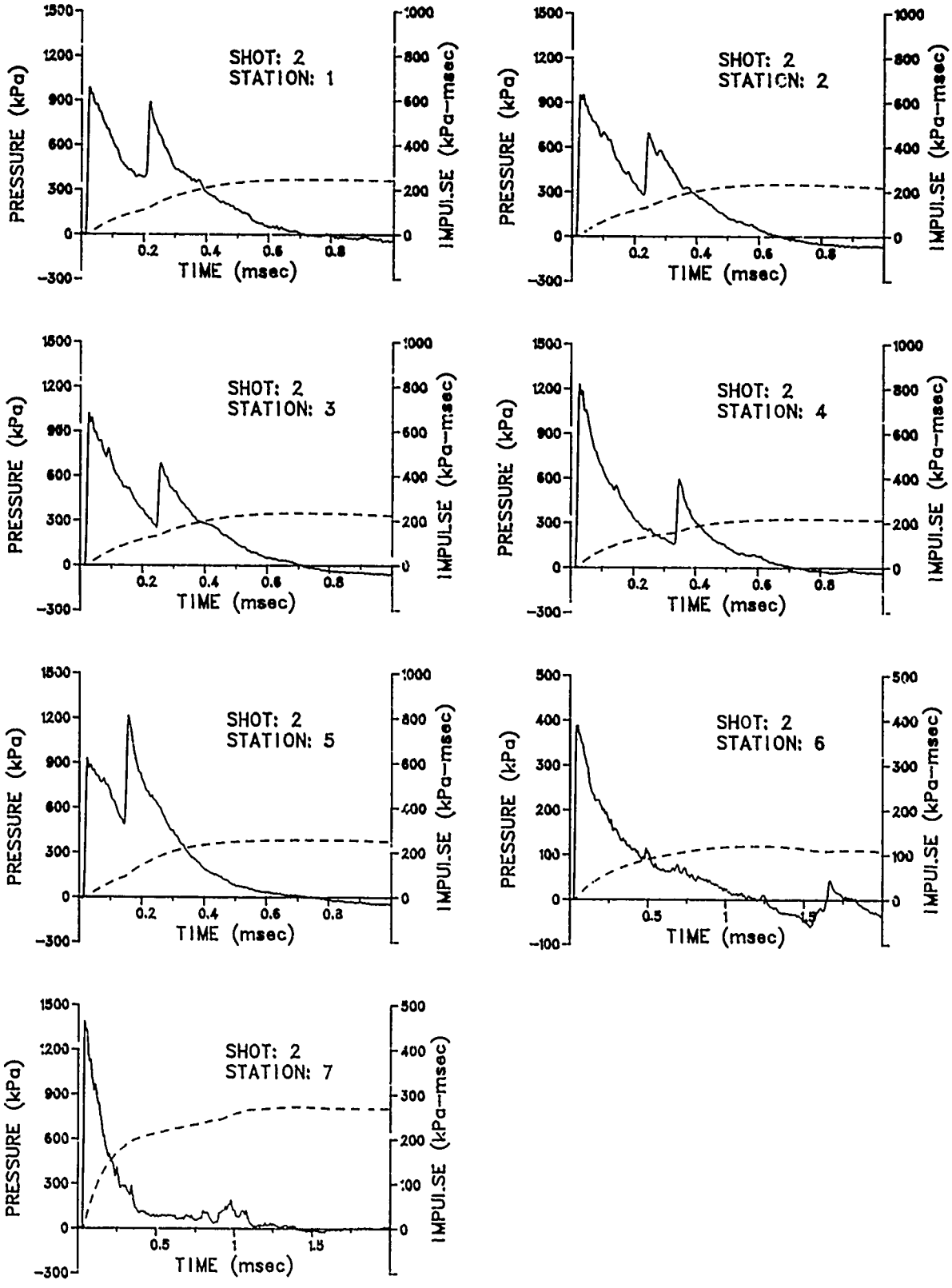

Figure 14. Pressure-time Histories for Shot 2

with the ground, is subjected to side-on pressure and monitors the blast wave propagating in front of the donor. Because the donor door was designed to fail, the blast was focused forward resulting in a peak pressure recorded at Station 7 that is close to side-on pressure for an unconfined 1 kg blast.

Stations 1 & 2 on Figure 14 both show an initial peak pressure of over 900 kPa followed by a lesser peak at 0.2 msec. The secondary peak is caused by a reflection of the shock wave from the ground. Stations 3-5 display similar twin peaks; in each case the relative magnitudes of the two peaks is determined by the distances from the wave sources. The blast wave strikes the upper edge of the wall first and decays as it travels downward to the ground line where it is reflected and travels upward, again decaying as a function of distance. For example, Station 4, located in the upper corner of the acceptor shows an initial peak of 1227 kPa and a 591 kPa secondary peak whereas Station 5, located in the lower corner much closer to the ground, shows a 927 kPa initial peak and a 1214 kPa secondary peak. Clearly, the peak pressure exhibited at Station 6, 388 kPa, is much lower. Station 7, the free field gage position, shows an initial pressure of 1388 kPa which is close to free field side-on pressure for an unconfined Pentolite charge, 1540 kPa (Reference 6).

The impulse for each gage position is also indicated on Figure 14. The impulse is a direct indication of the applied force and is used to calculate the maximum velocity for a freely translating wall which is the upper limit of obtainable velocities. As stated above, Stations 1 and 2 are of primary interest because the greatest fragment velocities should be obtained from the center of the wall. The peak impulses for Stations 1 to 5 are very close: 246.3, 233.7, 234.1, 217.9, and 256.3 kPa-msec. The average value is 237.7 kPa-msec. Peak impulse is defined as the impulse at the end of the blast wave positive phase duration.

For Shots 1-8 the donor structure, charge, and test pad were not varied; the blast loading should be the same for each shot. Therefore, the P-T records from Shot 2 are representative of all eight shots, and records for Shots 1 and 3-8 are presented in the Appendix.

Identical shots were also fired and are reported in References 2 and 5. The pertinent P-T records from those tests show that the blast data are self-consistent.

Peak pressure, impulse, shock arrival time, and positive phase duration for Shots 1-8 are listed in Table 2 for the primary stations of interest, Stations 1 & 2.

TABLE 2. AIRBLAST PARAMETERS FOR SHOTS 1-8

Shot#	Station#	Peak Pressure kPa (1st/2nd)	Impulse* kPa-msec	Arrival Time msec	Duration msec
1	1	1039.2 / 1034.2	276.7	0.9025	0.7050
1	2	800.6 / 621.2	212.4	0.8075	0.7050
2	1	983.9 / 889.3	246.3	0.8900	0.7025
2	2	949.7 / 693.6	233.7	0.8125	0.6725
3	2	884.3 / 873.1	231.0	0.8450	0.6650
4	2	**1091.7 / 850.6	263.1	-	0.6850
5	2	978.9 / 614.2	211.8	-	0.6725
6	2	1062.2 / 806.3	245.8	0.8250	0.6425
7	2	1009.9 / 819.1	258.6	0.8225	0.6800
8	2	***1002.7 / 862.9	257.7	0.8075	0.6825

* Impulse to end of positive phase
** Not considering the spike on Figure A-3
*** Not considering the spike on Figure A-7

The test pad layout was altered for Shot 9 by removing the barricades. Without the barricades to impede the shock wave, dynamic flow, and particle fragments, the blast loading on the near wall of the acceptors should be higher. Also, in this test arrangement, the shock wave strikes the near wall face-on which results in full reflected pressure. The P-T records for Shot 9 are displayed on Figure 15. These records may be compared with Shot 2 (Figure 14) which is an identical test except for the barricades. Comparison of Shots 2 & 9 shows the effects that the barricades have on attenuating the blast loading. Between Reference 2 and the current project, several configurations that are variations of the Machrihanish site have been tested; airblast parameters from these different configurations are presented in Table 3 to show the effects of the barricades and donor structure on confining the blast. Comparison is made at Station 3, a gage location used in each project. Station 4 was used for Shot 9, because it was difficult to measure blast pressure under such severe conditions. The record at Station 4 appears more realistic than that at Station 3. Table 3 lists blast environments from the least to the most severe. Evidently, loose sand barricades attenuate the blast more than hardpacked soil barricades. When the donor structure is removed, the blast pressure increases dramatically, but the impulse is not significantly increased. However, when the barricades are removed, both the pressure and impulse are markedly increased. The enhanced impulse is caused by particles striking the gage.

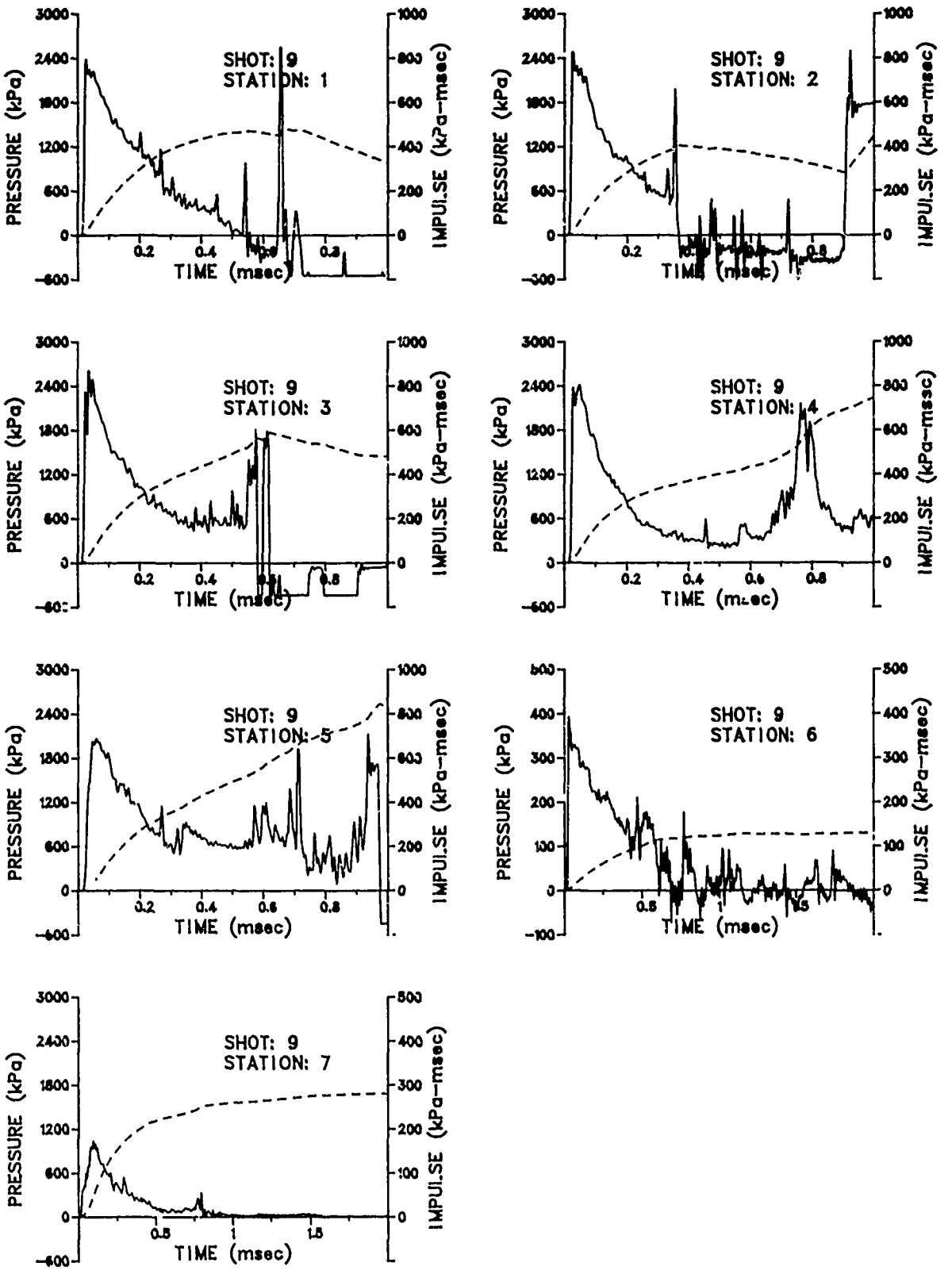

Figure 15. Pressure-time Histories for Shot 9

TABLE 3. EFFECTS OF BARRICADES AND DONOR STRUCTURE ON BLAST LOADING

Source	Station	Donor	Barricade	Pressure kPa	Impulse kPa-msec	Arrival Time msec	Duration msec
Ref. 2 Shot 3	3	Yes	Sand	821	195.0	0.8500	0.70
Shot 6	3	Yes	Soil	1079	245.8	0.8475	0.70
Ref. 2 Shot 4	3	Yes	Soil	1093	239	0.8900	0.71
Ref. 2 Shot 5	3	Floor Only	Soil	2015	240	0.5120	0.58
Shot 9	4	Yes	No	2387	746	1.025	1.1

B. Strength of the Concrete Acceptor Wall

A description of these tests may be found in Section II B 4.

1. Quasi-static Tests. Ten concrete walls of several preliminary designs were tested quasi-statically to obtain an initial approximation for a workable final design. The results of the tests are listed in Table 4. For a sample of eight walls having a mean mass of 0.90 kg, the distributed load required to crack the panels in tension was 34.4 kPa and the displacement to failure was 0.49 mm. As a matter of general interest, the displacement as a function of applied force for the unscored 0.92 kg wall is shown in Figure 16. The walls with the finest scoring pattern, 2.12 x 2.54 cm, failed at lower than the mean pressure, but for the most part, walls with the other scoring patterns did not crack more readily than unscored walls. The scores, when present, were shallow, having a nominal depth of 0.32 mm. The quasi-static tests showed that every concrete wall failed near enough to 34.5 kPa to be acceptable. Quasi-static tests on 1/40 scale brick walls composed of cement-lime mortar and red granite chips are reported in Reference 7 where wall failure occurred at 34.5 $\pm$20.7 kPa.

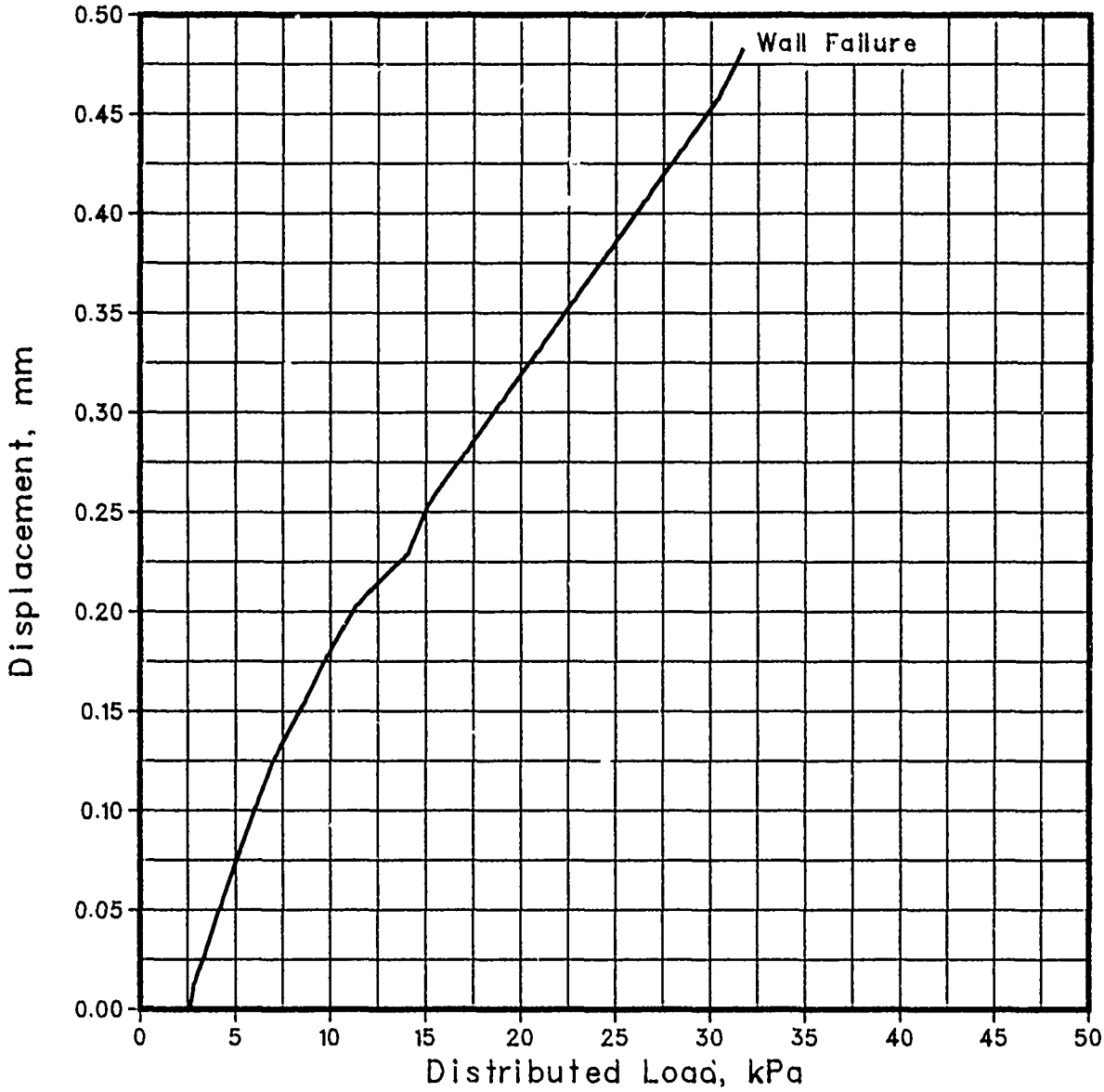

Figure 16. Displacement as a Function of Applied Force for an Unscored Wall

TABLE 4. CONCRETE WALL QUASI-STATIC STRENGTH TESTS

Mass (kg)	Distributed Load (kPa)	Displacement (mm)	Scoring Pattern (cm)	Curing Period (days)
0.92	31.8	0.48	None	19
0.86	36.4	0.43	None	36
0.86	40.5	0.43	4.66x5.08	29
0.91	33.0	0.58	4.66x5.08	26
0.92	32.6	0.51	4.66x5.08	26
0.90	47.8	0.56	4.66x2.54	19
0.90	28.4	0.46	2.12x2.54	22
0.90	25.0	0.46	2.12x2.54	22

Scoring the walls influenced the breakup pattern. An unscored panel exhibited predictable cracks (see Figure 17) for a wall under tension because of bending moment. A scored wall tended to crack along the scores (see Figure 18).

As a result of these static tests, a 2.54 x 2.54 cm scoring pattern was determined to be suitable for the field tests.

2. Dynamic Tests. Ten concrete walls were tested for strength in tension using the BRL 10.2 x 38.1 cm shock tube. The results are indicated in Table 5. All of the walls tested dynamically have a 2.54 x 2.54 cm scoring pattern except for one unscored wall. The walls were scored in one of two ways. In method I, the walls were scored immediately after being poured resulting in shallow, irregular scores, nominally 0.32 cm. In method II, the walls were allowed to set up for several hours and then scored. This resulted in deeper, regular scores, nominally 0.445 cm. Three driver lengths were used for these tests. The driver length determined the impulse and positive phase duration of the shock wave. The walls were exposed to full reflected pressure; the column labelled "Failure Range" in Table 5 indicates that a wall did not fail at the lower reflected pressure, but did fail at the higher value.

With the long driver installed, five walls tested failed at less than 22.8 kPa. With the medium length driver, two walls tested failed at less than 15.9 kPa. When the driver was shortened to 8.3 cm, 2 of 3 walls tested failed at higher pressure, between 21.4 and 31.7 kPa. The failed slabs showed both cracks caused by failure under tension and cracks caused by shear failure along the supporting edges. The dynamic tests showed that walls with a 2.54 x 2.54 cm scoring pattern would be workable for the field tests. Both the regularly and irregularly scored walls failed close enough to 34.5 kPa to be acceptable.

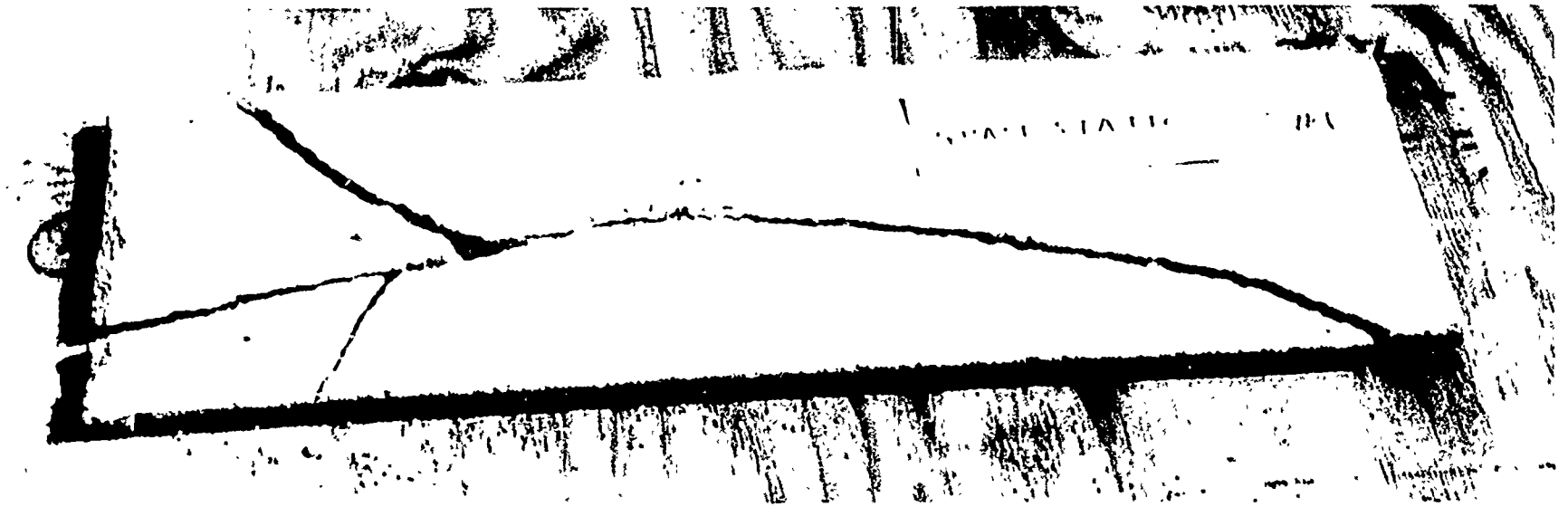

Figure 17. Breakup Pattern of a Quasi-statically Tested Unscored Concrete Wall

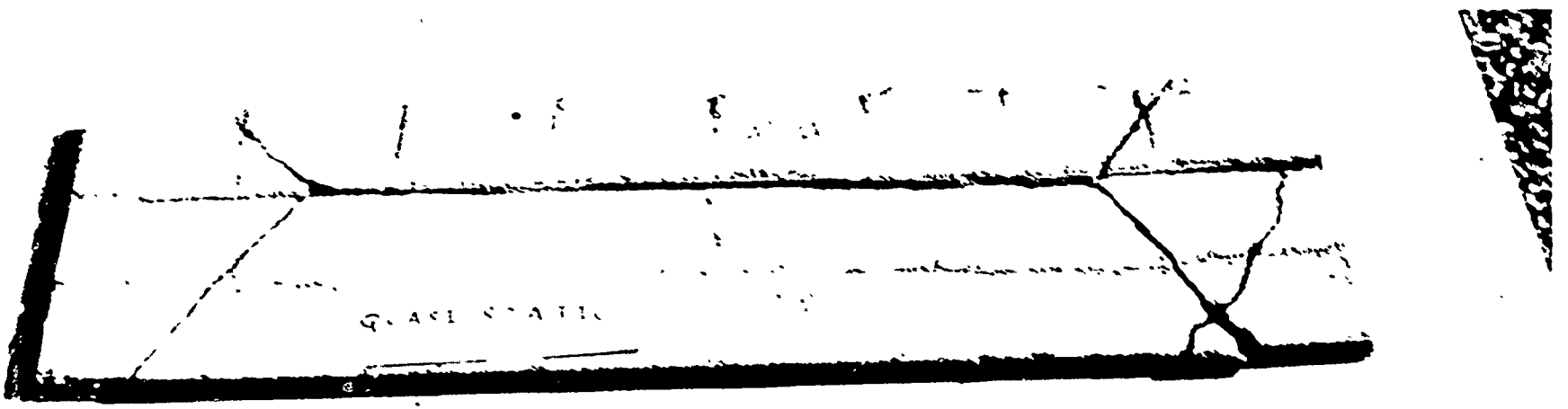

Figure 18. Breakup Pattern of a Quasi-statically Tested Scored Concrete Wall

TABLE 5. CONCRETE WALL DYNAMIC STRENGTH TESTS

Mass (kg)	Failure Range (kPa)	Driver Length (cm)	Load Duration (msec)	Scoring Pattern*	Curing Period (days)
0.96	<22.8	147.3	10	I	25
0.86	17.2-20.7	147.3	10	I	26
0.73	<13.8	147.3	10	I	19
0.77	<16.5	147.3	10	II	23
0.93	15.2-17.2	147.3	10	I	19
0.94	13.8-15.2	45.7	7	I	13
0.91	13.8-15.9	45.7	7	II	23
0.97	21.4-31.7	8.3	3.5	None	20
0.80	15.2-21.4	8.3	3.5	I	23
0.91	21.4-31.7	8.3	3.5	II	30

* I - shallow, irregular scores, nominally 0.32 cm
II - regular scores, nominally 0.445 cm

Apparently, the concrete wall is sensitive to the load duration. It is possible to calculate the fundamental frequency of vibration for the concrete wall if several assumptions are fulfilled (Reference 8). The wall is assumed to be elastic, homogeneous, isotropic , of uniform thickness, and the deflections are small in comparison with the wall thickness.

Let h = wall thickness
D = flexural rigidity of wall
E = modulus of elasticity in tension = 3,000,000 LB/sq in (Reference 9)
ν = Poisson's ratio = 0.13
d = weight per unit volume of material in the wall
g = gravitational acceleration
b = wall length
c = wall width
f = fundamental frequency of vibration

Then,

$$D = \frac{E h^3}{12 (1 - \nu^2)} \qquad (1)$$

and

$$f = \frac{\pi}{2} \left(\frac{1}{b^2} + \frac{1}{c^2}\right) \sqrt{\frac{gD}{hd}} \qquad (2)$$

From Equation 2, it was determined that the fundamental frequency equals 213.2 cycles per second, and the period of vibration is 4.7 msec. The data in Table 5 shows that for the load durations of 10 or 7 msec, the walls failed at lower pressures than for the load duration of 3.5 msec. The period of vibration, 4.7 msec, falls between 3.5 and 7 msec. Evidently, the data in Table 5 indicates that when the duration of the applied load exceeds the period of vibration of the wall, failure occurs at lower pressure than when the period exceeds the load duration. Perhaps under field test conditions, where the load is applied for only 0.7 msec, the wall may require overpressures higher than 34.5 kPa for failure.

C. Shock Tube Fragment Velocity Measurements

A decription of these tests was given in Section II C. The BRL 10.2 x 38.1 cm shock tube was used to simulate the blast loading expected in the field tests. Results from Reference 2 were used to predict the blast loading for the field tests reported in this study. Specifically, air blast parameters from Shot 4, Station 3, of Reference 2, which are listed in Table 3 of this report, were used. That record shows 1093 kPa peak pressure, 239 kPa-msec impulse, and 0.71 msec duration. In these shock tube tests it was not possible to reproduce such a high pressure, short duration pulse. The best approach was to match the impulse by creating a 80.0 kPa peak pressure wave of 7.4 msec duration. This resulted in an impulse of 224.5 kPa-msec which is close to the field case. Two walls and two 2.54 cm concrete plugs were tested in this arrangement. The results are listed in Table 6. Since no energy was needed to free the plugs, their velocities are higher than wall fragment velocities. The velocities are very low, the highest value being 11.4 m/s. The vertical velocity as a result of gravity is about 1 m/s; this is not indicated on Table 6.

TABLE 6. SHOCK TUBE FRAGMENT VELOCITY MEASUREMENTS

Target*	Mass (kg)	HORIZONTAL Velocity (m/s)	CURING Period (days)
I	0.88	7.0	17
II	0.90	5.0	39
Plug	0.00595	10.0	39
Plug	0.00595	11.4	39

* I - wall having shallow, irregular scores
II - wall having regular scores

D. Field Tests Fragment Velocities

1. Data Analysis. The velocity data for nine field shots are presented in Table 7. Velocity measurements were recorded for fragment movement from the back of the near sidewall to a position 9.6 cm from the near sidewall (4.5 cm from the centerline of the model). Several independent circuits were set up to record independent velocity measurements. The measurements obtained from the independent circuits were consistent. When more than one valid measurement was obtained, the value listed in Table 7 is the highest value. The raw velocity data is actually a little lower than the true velocity because it takes the load duration, 0.7 msec, for the fragments to accelerate to maximum speed. During the loading time, the wall has moved 6.3 mm on average based on the equations of motion discussed below. Also, the value recorded by the counters is the horizontal velocity; including gravitational acceleration and any vertical component of the applied load increases the velocity slightly.

The last column of Table 7, labelled "Classical Limit", indicates the maximum velocity a target could reach as a result of an applied load. This value was calculated by using the pressure-time records as input to a computer program that calculated the force applied to the target as a function of time. The assumptions made are that the target translates freely, that is, no blast energy is used to break it up, and the entire blast wave applies a force to the target, that is, the load is applied before the target breaks up. These basic equations of motion are included for completeness.

Let M = target mass
a = instantaneous target acceleration
F(t) = applied force on target as a function of time
p(t) = blast pressure on target as a function of time
A = target cross-sectional area
dt = pressure record time increment (digitizing time step)
dv = instantaneous target velocity

Then,

$$F(t) = A\ p(t) \tag{3}$$

$$a = \frac{F(t)}{M} = \frac{dv}{dt} \tag{4}$$

$$v = \int a\ dt \tag{5}$$

and the final velocity may be computed by numerically integrating the velocities from shock arrival until the end of the positive phase. The upper limit velocity as a function of time for the concrete wall used on Shot 6 is displayed graphically on Figure 19.

TABLE 7. FIELD TEST VELOCITY DATA

Shot#	Target	Mass (kg)	Scoring Pattern*	Measured Velocity (m/s)	Classical Limit (m/s)
1	Plug	0.0065	-	-	21.6
2	Plug	0.00635	-	6.3	19.7
3	Wall	0.81	II	10.8	14.6
4	Wall	0.95	II	8.5	14.3
5	Wall	0.98	II	6.6	11.2
6	Wall	0.82	I	10.8	15.5
7	Wall	0.94	I	8.0	14.2
8	Wall	0.96	None	4.7	13.9
9	Plug	0.0028	-	35.8	21.4
	Plug	0.00635	-	124.6	37.2

* I - wall having shallow, irregular scores
II - wall having regular scores

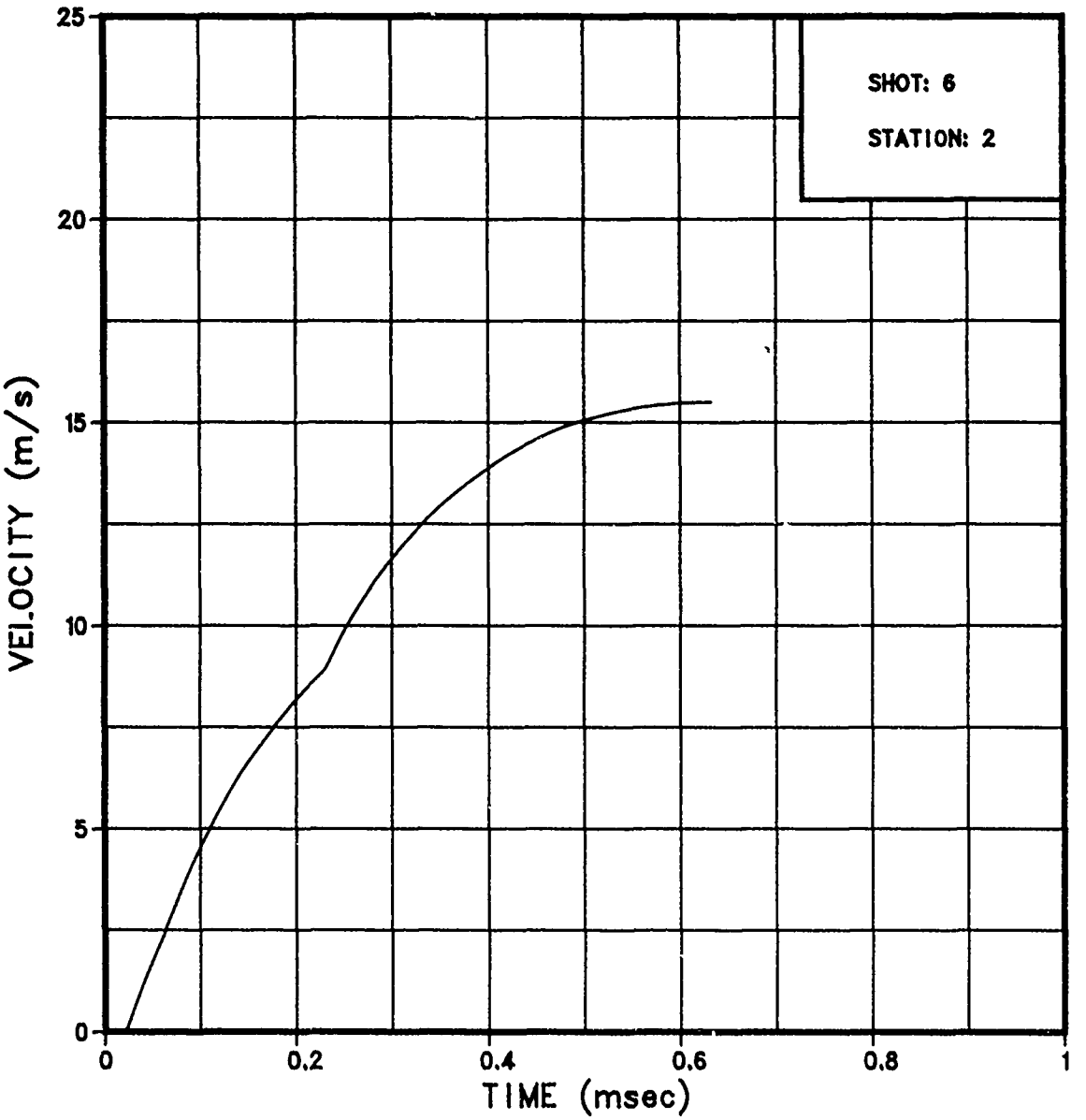

Figure 19. Velocity vs. Time for a Freely Translating 0.82 kg Concrete Wall Using Shot 6, Station 2 as the Applied Load

For the six shots where walls were tested, the measured velocities ranged from 4.7 m/s minimum for an unscored wall to 10.8 m/s maximum for the scored walls. Using Equation 5, the calculated upper limit velocities for walls were in the range 11.2-15.5 m/s. These calculations were based on Station 2, at the center of the nonresponding sidewall, for each shot where a wall was tested. There are several reasons why the measured velocities are lower than the limiting velocities. As previously indicated the true velocity is slightly greater than the measured velocity, because the fragments are accelerating for approximately 0.7 msec while the load is being applied. Furthermore some blast energy is required to breakup the wall; this energy will not accelerate the wall. Also, not all of the blast energy that reaches the fragment will go into fragment motion. Some portion of the blast wave will be diffracted around the fragments.

On Shot 1 valid measurements were not recorded. On Shot 2, a velocity of 6.3 m/s for a 6.35 gram plug was measured. This value is lower than the wall velocities, because the shock wave strikes the plug at a 33.9 degree angle and pushes the plug against its support instead of driving the plug straight through the hole. The upper limit velocity for the plug, 19.7 m/s, is higher than that for walls, because this plug is thinner than the wall and requires less applied force to propel it.

On Shot 9 the barricades were removed. The measured velocities of 35.8 and 124.6 m/s are not considered reliable. These could be measurements of the plugs or blast debris. Likewise, the upper limit velocities for Shot 9 are based on erratic pressure-time histories.

2. Comparisons. In Reference 1, Ward and Porzel used air blast parameters to analytically derive the blast load impinging on the center of the near sidewall of a Machrihanish magazine. The method used to derive the loading profile is discussed in the triservice manual, "Structures to Resist the Effects of Accidental Explosions" (Reference 10). There are several different magazine designs at Machrihanish; the magazine modeled in Reference 1 is 7.62 x 6.10 x 3.05 meters which is smaller than the magazine discussed in this report. Using the equations of motion, the idealized blast load was applied to a unit area fragment of the near sidewall. It was determined that the maximum velocity of a near sidewall fragment would be 58 m/s. These computations do not consider any blast shielding effects produced by the barricades.

Velocity measurements of fragments from 1/8 and 1/40 scale brick walls subjected to a blast wave are reported by Raynham (Ref. 7). The models were exposed to a 100 ton TNT blast; they were placed at the 66.2 kPa and 89.6 kPa side-on pressure level. The 1/8 scale walls were composed of 2.7 x 1.27 x 0.9 cm model bricks joined with a cement-lime mortar. The 1/40 scale walls were an amalgam of cement-lime mortar and red granite chips that simulated standard bricks on the 1/40 scale. Raynham concludes that for the 1/8 scale walls the mean velocity of the large fragments at the 89.6 kPa level is 16.2 m/s and at the 66.2 kPa level is 11.5 m/s. Similarly, for the 1/40 scale walls the mean velocity of the large fragments at the 89.6 kPa level is 19.4 m/s and at the 66.2 kPa level is 14.3 m/s.

IV. CONCLUSIONS

The fragment velocities measured in this 1/23.5 scale model experiment indicates that the mass detonation of one magazine would not cause a sympathetic detonation in the nearest neighbor magazine. The velocities measured were in the range of 4.7 - 10.8 m/s. Reference 1 has a discussion of the velocities required for munition detonation. Virtually all explosives of interest are safe from exposure to massive debris at 60 m/s.

ACKNOWLEDGEMENTS

The authors wish to thank all the players involved in this project. John Sullivan assisted in planning and implementing the quasi-static tests. Dominick DiBerardo performed the quasi-static tests, improvising all the way. Kenneth Holbrook, the charge handler and field technician, kept the field tests running smoothly. Bud Dunbar did his usual excellent job as recording engineer. Alan Trowbridge, of Dynamic Sciences, Inc., showed considerable skill in obtaining valid velocity measurements by modifying the break screen setup to accommodate blast effects. The assistance of Dynamic Sciences, Inc. was provided by the Velocity Measurements Branch of the Combat Systems Test Activity.

REFERENCES

1. F. B. Porzel, J. M. Ward, "Explosive Safety Analyses of the Machrihanish Magazine," NSWC TR 79-359, December 1979.

2. C. N. Kingery, G. Bulmash, P. Muller, "Blast Loading on Above Ground Barricaded Munition Storage Magazines," BRL TR 2557, May 1984 (AD A141677).

3. "The Effects of Nuclear Weapons," Department of the Army Pamphlet No. 50-3, March 1977.

4. G. A. Coulter, B. P. Bertrand, "BRL Shock Tube Facility for the Simulation of Air Blast Effects," BRL MR 1685, August 1965, (AD 475669).

5. G. A. Coulter, C. N. Kingery, P. Muller, "Blast Loading on Above Ground Barricaded Munition Storage Magazines-II," BRL TR-2694.

6. Private Communication.

7. C. J. Raynham, "Model Studies of the Movement of Debris from Brick Panels which Fail under the Action of a Blast Wave," United Kingdom Atomic Energy Authority, AWRE Report E 7/63, March 1963.

8. L. S. Marks, Mechanical Engineers' Handbook, seventh edition, McGraw-Hill, 1967.

9. R. J. Roark, Formulas for Stress and Strain, second edition, McGraw-Hill, 1943.

10. Departments of the Army, Navy, and Air Force, "Structures to Resist the Effects of Accidental Explosions," TM 5-1300, NAVFAC P-397, AFM 88-22, June 1969.

APPENDIX

PRESSURE-TIME RECORDS FOR SHOTS 1 AND 3 TO 8

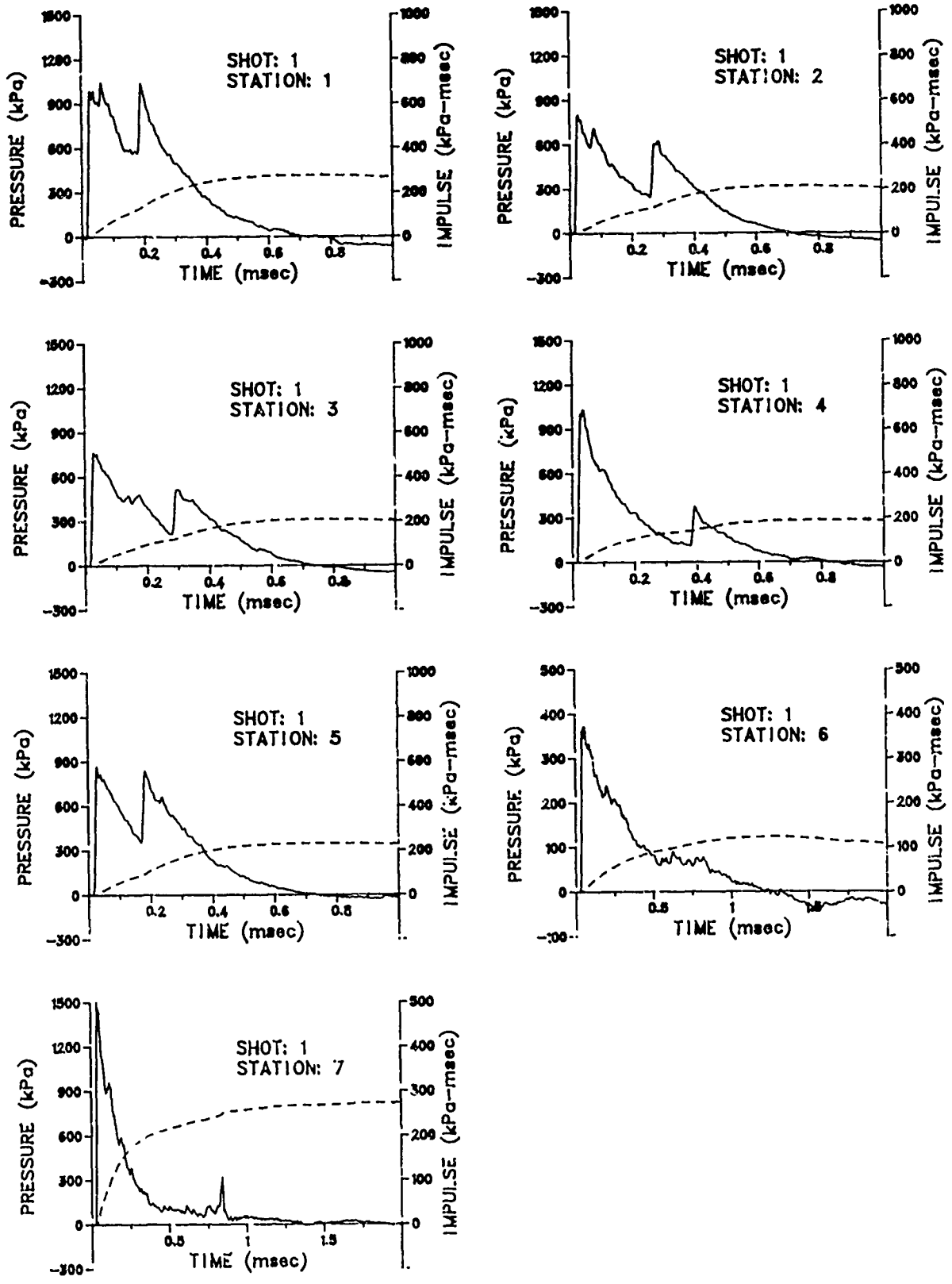

Figure A-1. Pressure-time Histories for Shot 1

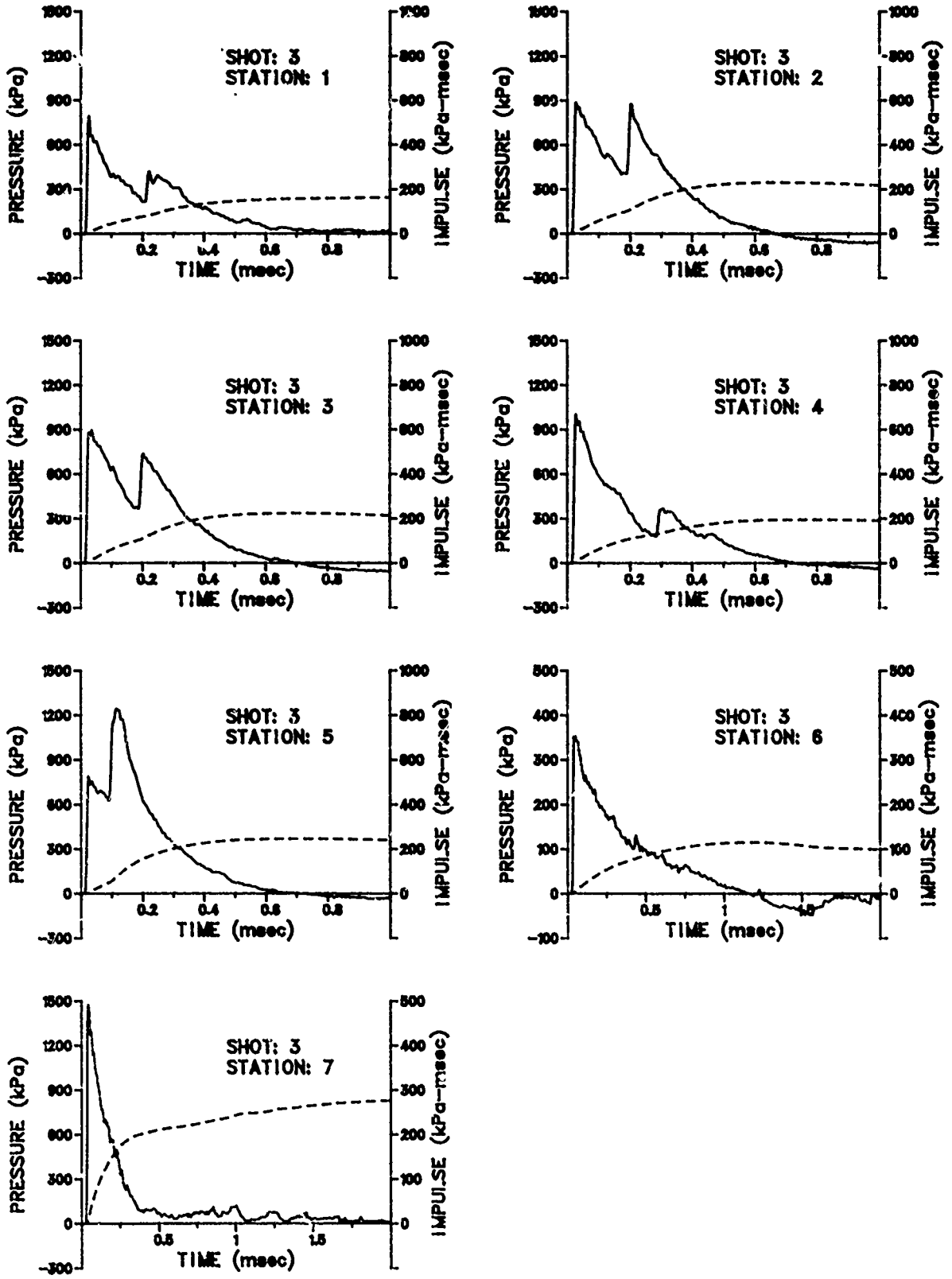

Figure A-2. Pressure-time Histories for Shot 3

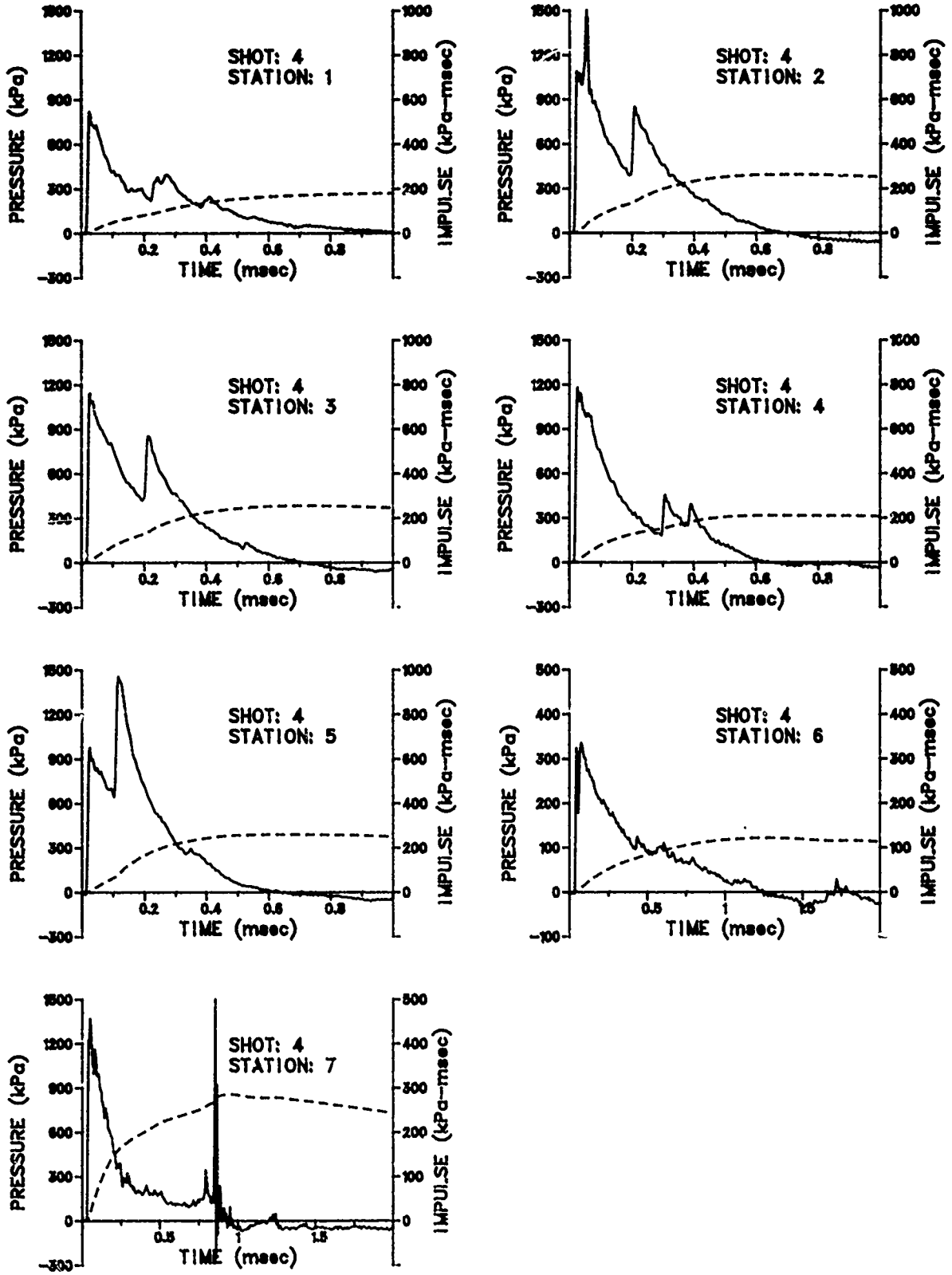

Figure A-3. Pressure-time Histories for Shot 4

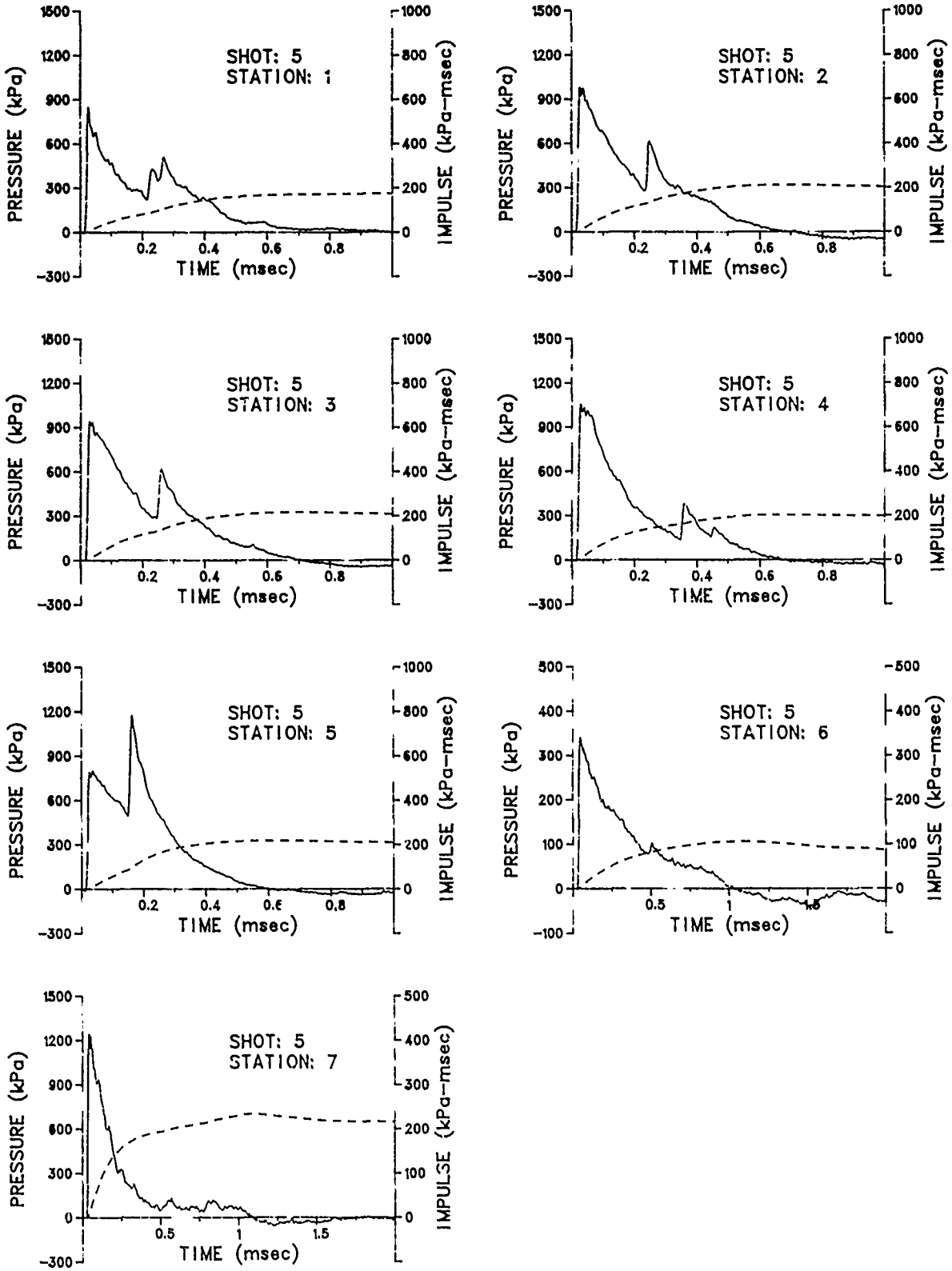

Figure A-4. Pressure-time Histories for Shot 5

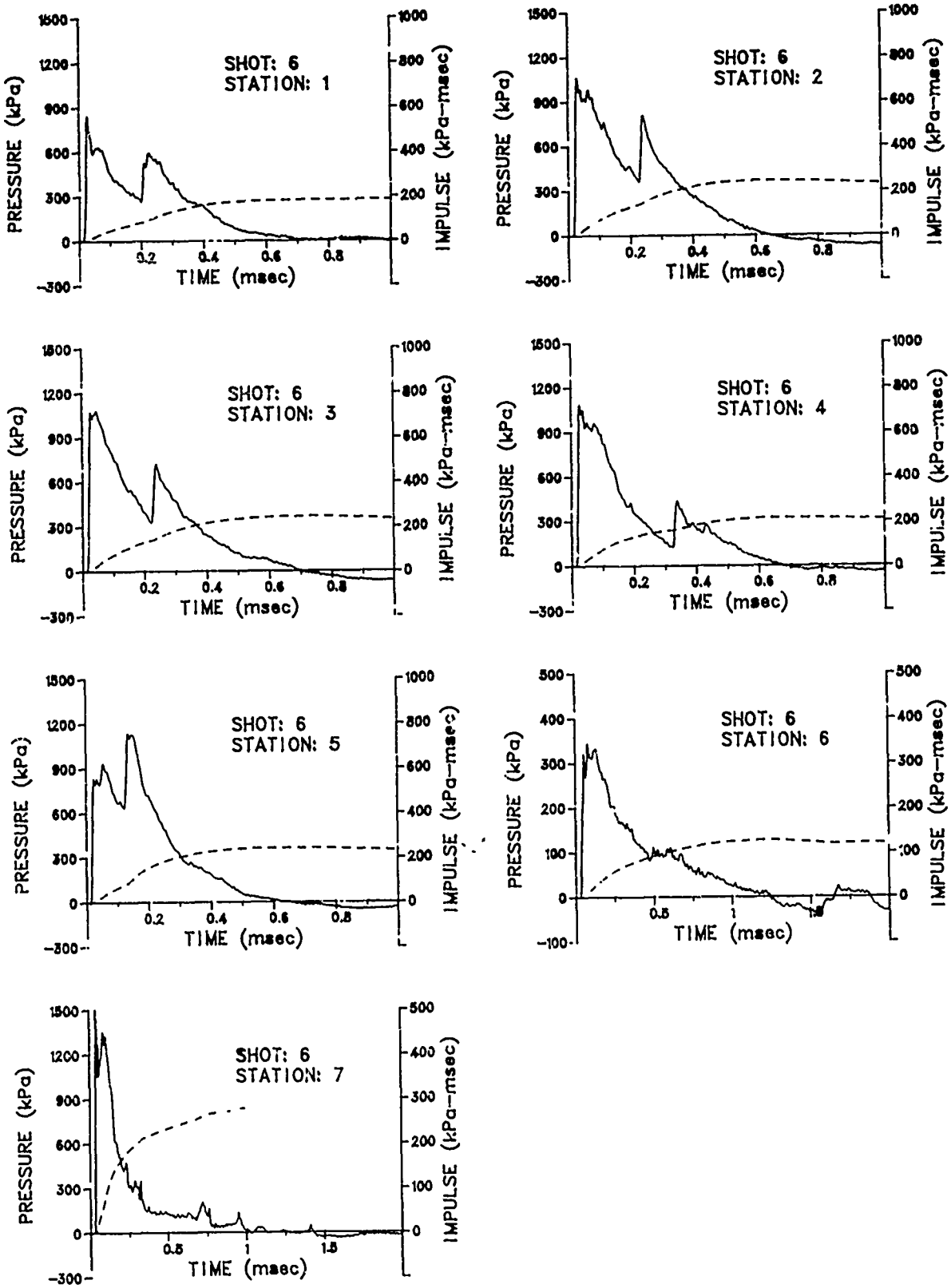

Figure A-5. Pressure-time Histories for Shot 6

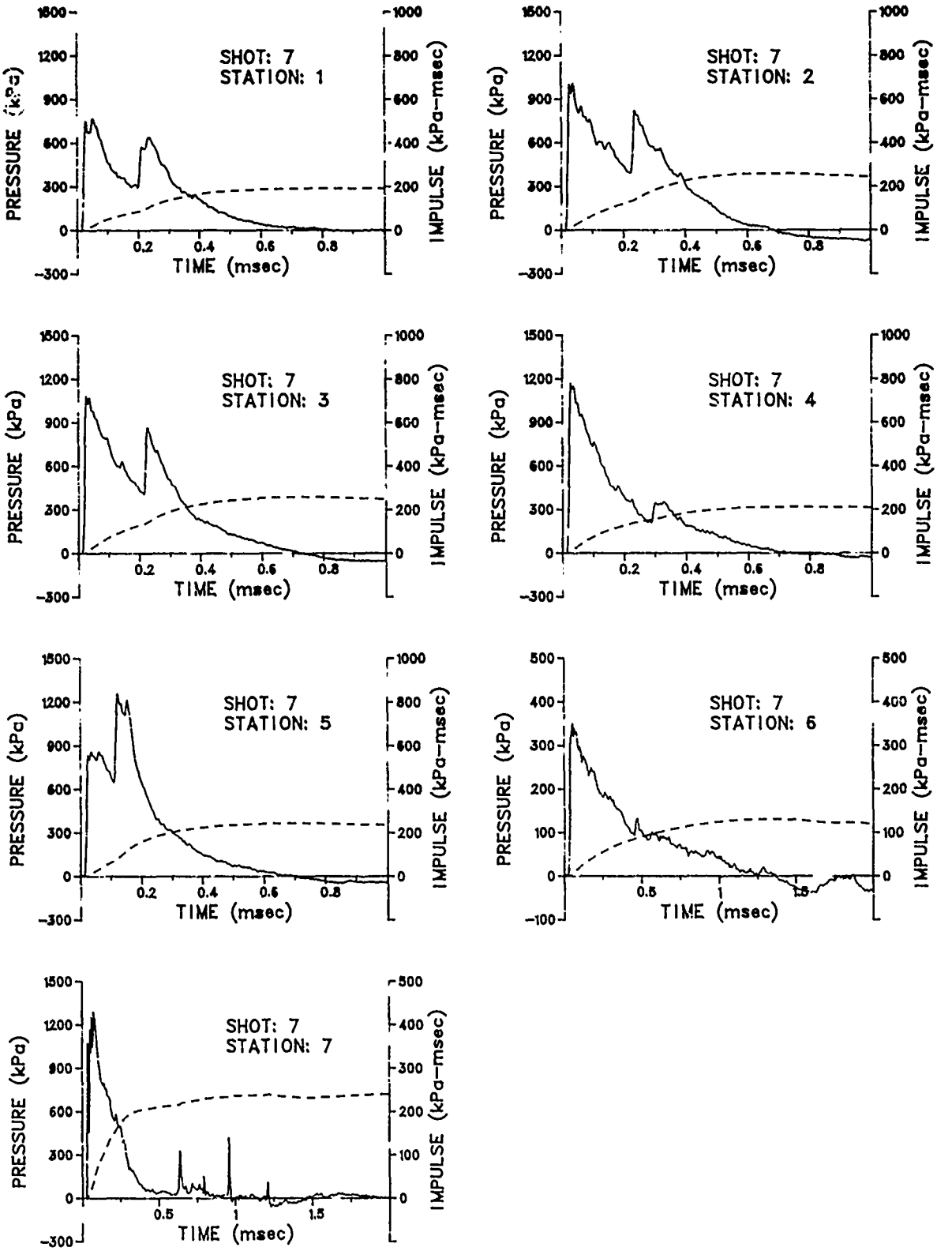

Figure A-6. Pressure-time Histories for Shot 7

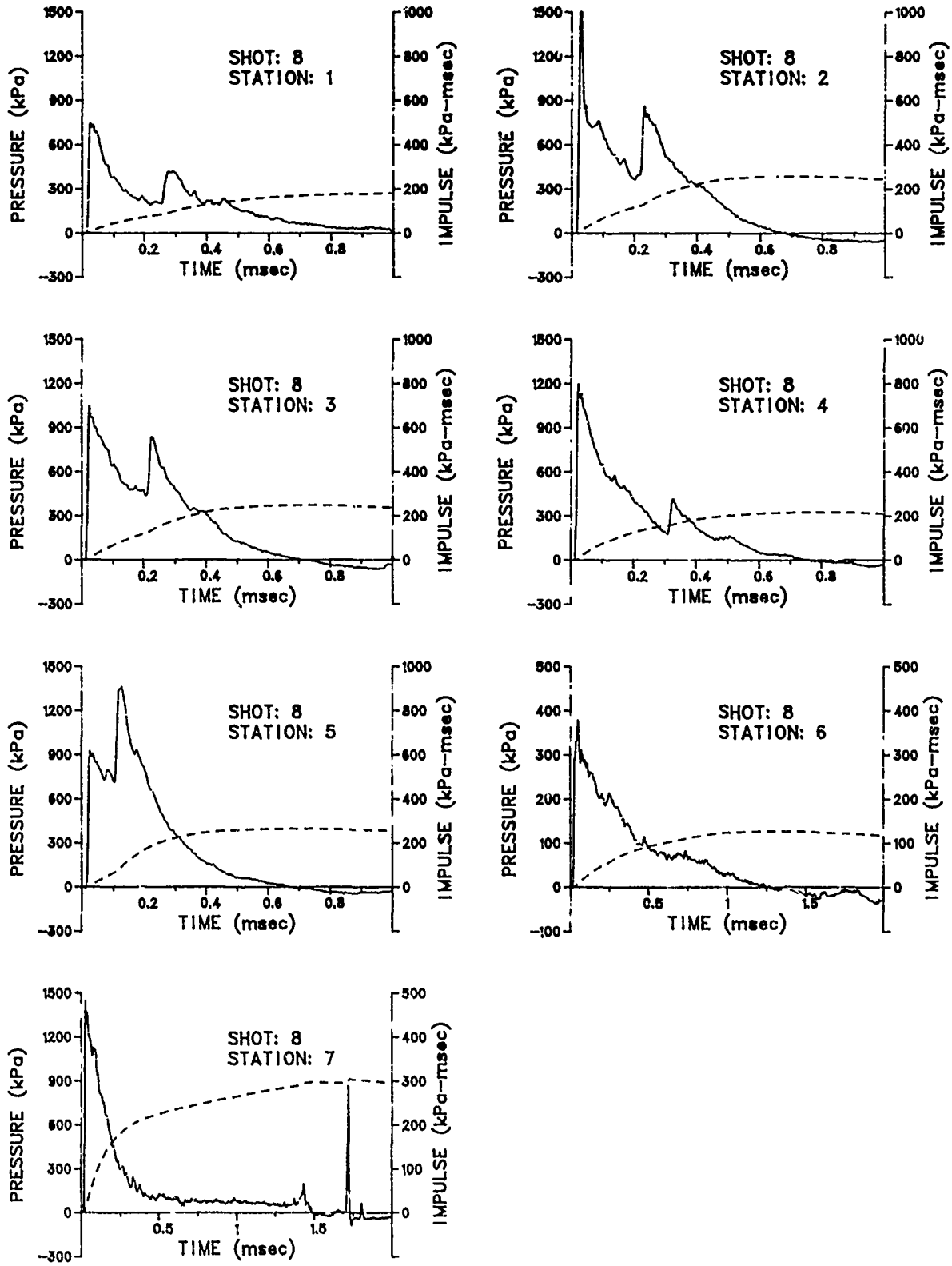

Figure A-7. Pressure-time histories for Shot 8